Agricultural Research D
Winand Staring Centre for Integrated Land, Soil and Wate

Modelling of soil acidity and nitrogen availability in natural ecosystems in response to changes in acid deposition and hydrology

J. Kros, G.J. Reinds, W. de Vries, J.B. Latour

and M.J.S. Bollen

sc-dlo

rivm
onderzoek in dienst
van mens en milieu

REPORT 95
Wageningen (The Netherlands), 1995

Modelling of soil acidity and nitrogen availability in natural ecosystems in response to changes in acid deposition and hydrology

J. Kros
G.J. Reinds
W. de Vries
J.B. Latour
M.J.S. Bollen

Report 95

DLO Winand Staring Centre, Wageningen (The Netherlands), 1995
RIVM National Institute of Public Health and Environmental Protection

ABSTRACT

J. Kros, G.J. Reinds, W. de Vries, J.B. Latour, M.J.S. Bollen, 1995 *Modelling of soil acidity and nitrogen availability in natural ecosystems in response to changes in acid deposition and hydrology* Wageningen (The Netherlands), DLO Winand Staring Centre. Report 95. 90 pp.; 9 Figs; 25 Tables; 81 Refs; 3 Annex.

Changes in vegetation are often caused by changes in abiotic site factors. The SMART2 model has been developed to evaluate the effects of changes in ion inputs by atmospheric deposition and seepage on these site factors. Linkage with the Multiple Stress Model for Vegetation (MOVE) enables the effects on the occurrence probability of vegetation species in response to deposition and seepage scenarios to be evaluated. Combinations of two deposition and two seepage scenarios were evaluated with SMART2. Results focused on pH, nitrogen availability and base saturation. Effects of changes in pH on the occurrence probability of forest understorey in a nutrient-poor deciduous forest were evaluated with MOVE.

Keywords: drought, eutrophication, nutrient cycling, soil acidification, vegetation

ISSN 0927-4499

Project 7305 [Rep95.HM/04.96]

Contents

Tables

Figures

Preface

To evaluate the effects of changes in pH, nitrogen availability and mean spring water-table on the occurrence probability of individual plant species, the Multiple stress mOdel for VEgetation (MOVE) was developed at RIVM. In order to evaluate changes in soil pH and nitrogen availability in response to acidification, man-induced drought and eutrophication scenarios, RIVM asked SC-DLO to extend the SMART model towards a module that can serve as soil module for the MOVE model. The model thus derived is called SMART2. Model extensions, data derivation and applications were carried out at SC-DLO, whereas most of the GIS work was accomplished at RIVM. With the release of the combination SMART2/MOVE an instrument came available for evaluating the effects of acidification, eutrophication and drought on the occurrence probability of individual plant species on a national scale. In addition, the SMART2 module was also developed to serve as a soil module within the regional applicable integrated model for the development of wilderness areas (GREINS). The GREINS model is being developed as a concerted action of AB-DLO, IBN-DLO and SC-DLO.

This research was financially supported by RIVM within the framework of the project 'Gebiedsgerichte Integratie' and the Ministry of Agriculture, Nature Management and Fisheries. We thankfully acknowledge the following colleagues for their efforts: Igor Staritsky, Jan Diesel, Rinke Heida and Theo Thewessen from RIVM for building an interface towards INGRES and the installation of the software at RIVM; Rien Pastoors from RIVM for providing data from the National Groundwater Model (LGM); Jan-Cees Voogd from SC-DLO for his assistance in data processing; Max Posch and Hans van Grinsven from RIVM for their comments. Finally, the National Spatial Planning Department is gratefully acknowledged for providing the National Survey on Landscape Ecology.

The authors

Summary

To quantify site factors, such a pH and nutrient availability, in natural ecosystems in response to various environmental control strategies, the SMART2 model has been developed. The objective was to provide a simple, nationally applicable model to gain insight into the effects of seepage, atmospheric deposition and nutrient cycling on terrestrial ecosystems. The SMART2 model was derived from a dynamic soil acidification model SMART (Simulation Model for Acidification's Regional Trends), which has been developed to evaluate the effectiveness of emission control strategies for SO_2, NO_x and NH_3 on a European scale. SMART is a simple one-compartment model which only includes geochemical buffer processes (e.g. weathering and cation exchange). The major enhancements in SMART2 are the inclusion of a biocycle and an improved modelling of hydrology, including solute input through upward seepage.

The SMART2 model is linked to the Multiple stress mOdel for VEgetation (MOVE). MOVE has been developed to predict the probability of occurrence of individual plant species as a function of the acid, nutrient and moisture status of the soil. Within the integrated SMART2-MOVE model, SMART2 forms the link between the environmental scenarios and the abiotic site factors, affecting the occurrence probability of plant species. With the integrated SMART2-MOVE model a relatively simple tool became available for the evaluation of the combined effects of environmental scenarios on the occurrence probability of plant species on a national scale.

For the Netherlands various acidification and seepage scenarios (1990-2050) were evaluated with SMART2. The results are focused on pH and nitrogen availability. Calculations were made for combinations of five vegetation structures (three forest types, heather and grass) on seven soil types (three sandy soils, two clay soils, peat and loess soils) and five water-table classes, using a 1 x 1 km^2 grid. Effects of changes in pH, as calculated with SMART2, on the occurrence probability of forest understorey in a nutrient poor deciduous forest were evaluated with MOVE.

Results showed that reductions in acid atmospheric deposition lead to a relatively fast improvement of the site factors, characterized by an increase in pH and base saturation and decrease in N availability. A reduction in groundwater abstractions by 25% has little or no effect on the pH and N availability, because the effect of reduction in groundwater abstractions on the seepage fluxes is almost negligible. Effects of the deposition reductions on the occurrence probability of forest understorey in a nutrient poor deciduous forest show an increase of the average predicted number of species from 40 to 80% in 1990 to 60 to 100% in 2050.

1 Introduction

Changes in vegetation are often caused by changes in abiotic site factors, such as pH and nitrogen availability. It has been recognized that abiotic site factors are affected by atmospheric deposition and water-table changes. Changes in abiotic site factors may cause threats to the structure and functioning of (semi-natural) ecosystems, and thus to the earth's biodiversity. In practice changes, which may cause threats, in site factors occur simultaneously. As a result ecosystems are affected by various threats (multiple stress effect). Research on environmental effects on ecosystems, however, is generally confined to one stress exclusively. Besides environmental effects site factors are also influenced by natural vegetation succession, vegetation management and land use changes.

Since the early eighties has been recognized that Dutch ecosystems receive large inputs of NH_4^+ and SO_4^{2-}, affecting soil solution concentrations, pH and nitrogen availability (Van Breemen *et al.*, 1982). Effects of enhanced atmospheric deposition of sulphur and nitrogen can be divided into: (i) (soil) acidification, leading to enhanced leaching of base cations, and in poorly buffered soils to increased dissolution of aluminium, resulting in unfavourable Al^{3+} concentrations and Al^{3+}/Ca^{2+} ratios, and (ii) eutrophication (caused by nitrogen only). In addition, enrichment with nitrogen in wet ecosystems is also due to increased input of eutrophicated groundwater and surface water. A thorough review of the impacts of N inputs on (semi-)natural ecosystems, i.e. bogs and wetlands, species-rich grasslands, heathlands and forest, related to vegetation changes, is given in Bobbink *et al.* (in prep.).

Research on forests indicated that increased nitrogen inputs cause high concentrations of NH_4^+ and NO_3^- in the soil solution (Roelofs *et al.*, 1985; Kleijn *et al.*, 1989), associated with a shift towards nitrophilous grass-species in the forest understorey (Hommel *et al.*, 1990). In addition, acidification (pH decrease) may also result in the decline of the original ground vegetation (Bobbink *et al.*, in prep.). Besides vegetation changes, increased nitrogen input and acidification may lead to: (i) nutrient imbalances, resulting from an increase in biomass, causing an increased demand of base cations (Ca^{2+}, Mg^{2+}, K^+) and the counteracting effect of reduced uptake of these cations due to increased NH_4^+ concentrations (Boxman and Van Dijk, 1988) and (ii) increased susceptibility to secondary stress factors such as frost (Aronsson, 1980) and infestations by fungi (Roelofs *et al.*, 1985).

Research on heathlands suggests that high inputs of atmospheric nitrogen are a significant factor in the transition of heathland to grassland (Heil and Diemont, 1983). Apart from the changes in competitive interactions between heather and grasses, heather beetle plagues, and nitrogen accumulation in the soil are important factors in vegetation changes in heathlands (Berdowski and Zeilinga, 1987; Berendse *et al.*, 1989). Generally, endangered species grow on soils with a higher pH, lower nitrogen content, and lower Al^{3+}/Ca^{2+} ratio (Bobbink *et al.*, in prep.).

Semi-natural species-rich grasslands are mostly deficient in nitrogen or phosphorus. Consequently, increased nitrogen availability will most likely lead towards highly

productive crop grasses and a decrease in species diversity (Bobbink *et al.*, in prep.). Wetland ecosystems showed also a significant decrease in diversity at elevated nitrogen inputs (Vermeer and Berendse, 1983).

In the Netherlands many vegetation types are phreatophytic because of the shallow water-table. In the last decades, these vegetation types have been suffered severely from lowering of the water-table, due to intensified drainage and groundwater abstractions (Van Amstel *et al.*, 1989). In addition, Hendriks (1994) showed that 29% of the Dutch forests suffers from drought. Apart from groundwater quantity, the seepage water quality has an important impact on species diversity in wetland ecosystems (Van Wirdum, 1991).

In order to evaluate the effect of eutrophication, acidification and drought, Latour and Reiling (1991) developed a conceptual, species-centred, Multiple stress mOdel for VEgetation (MOVE). MOVE is based on a risk assessment concept, which is used for various environmental problems to quantify ecological threshold values that correspond to defined protection levels for ecosystems. MOVE calculates the occurrence probability of plant species as a function of three abiotic site (soil) factors: pH, nitrogen availability and mean spring water-table. Because combined samples of vegetation and site factors are rare, the indication values of plant species by Ellenberg *et al.* (1991) are used to assess the site factors. Deduction of values for site factors from the vegetation guarantees ecological relevance. Combined samples of vegetation with site factors are used to calibrate Ellenberg's indication values with quantitative values of the abiotic site factors (Wiertz *et al.*, 1992).

To evaluate soil pH and nitrogen availability in response to acidification, drought and eutrophication scenarios, however, no model was directly available/suitable. Therefore it was necessary to derive a separate soil model for the evaluation of abiotic site factors.

The major objectives of this research were (i) to provide a simple, national applicable model to gain insight into the effect of seepage, acid deposition and nutrient cycling on terrestrial ecosystems and (ii) an indicative application of the model on a national scale. Therefore it was intended to extend the SMART model (De Vries *et al.*, 1989) towards a module that can serve as soil module for the MOVE model. Figure 1 shows the general concept of the integrated SMART-MOVE model. SMART is a dynamic soil acidification model, that has been developed to evaluate the effectiveness of emission control strategies for SO_2, NO_x and NH_3 on a European scale. SMART is a simple one-compartment model which only includes geochemical buffer processes (a.o. weathering and cation exchange). In order to model abiotic site factors in both dry and wet natural ecosystems the model was extended with a biocycle and an improved modelling of hydrology, including upward solute transport.

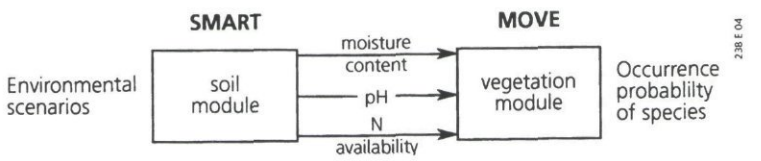

Fig. 1 Schematic presentation of the integrated SMART-MOVE model

With the combination of the extended SMART model and the MOVE model it should be possible to evaluate the response of site factors of terrestrial ecosystems to deposition and seepage scenarios to (i) assess the effectiveness of the combination of emission-deposition reductions and reduction in groundwater abstractions on a national scale, and (ii) identify areas with a large occurrence probability of specific plant species.

This report provides an overview of the necessarily adaptions of the SMART model, geographical information and data for a national application and an indicative application using one deposition scenario and one seepage scenario. Attention is also given to a model validation and the effect of uncertainty in model structure and input data on model results.

2 Model description

2.1 The original SMART model

2.1.1 Model structure

The original SMART model (De Vries *et al.*, 1989) consists of a set of mass balance equations, describing the soil input-output relationships, and a set of equations describing the rate-limited and equilibrium soil processes (Table 1). All major ions have been included. BC^+ (Na^++K^+) and Cl^- are only included in the charge balance.

Table 1 The processes and process descriptions included in SMART

Process	Element	Process description
Input		
Total deposition	SO_4^{2-}, NO_3^-, NH_4^+, BC^{2+} [1], BC^+ [2]	Inputs
Rate-limited reactions:		
Growth uptake	BC^{2+} [1], BC^+ [2], NH_4^+, NO_3^-	Constant growth
N immobilization	NH_4^+, NO_3^-	Proportional to N deposition and as a function of the C/N ratio
Nitrification	NH_4^+, NO_3^-	Proportional to net NH_4^+ input
Denitrification	NO_3^-	Proportional to net NO_3^- input
Silicate weathering	Al^{3+}, BC^{2+}, BC^+	Zero order reaction
Equilibrium reactions:		
Dissociation/association	HCO_3^-	CO_2 equilibrium equation
Carbonate weathering	BC^{2+}	Carbonate equilibrium equation
Al hydroxide weathering	Al^{3+}	Gibbsite equilibrium equation
Cation exchange	H^+ [3], Al^{3+}, BC^{2+}	Gaines Thomas equations
Sulphate sorption	H^+, SO_4^{2-}	Langmuir equation

[1] BC^{2+} stands for divalent base cations (Ca^{2+}, Mg^{2+})
[2] BC^+ stands for monovalent base cations (K^+, Na^+)
[3] Implicitly, H^+ is affected by all processes. This is accounted for by the charge balance

SMART was constructed using a process-aggregated approach, to minimize the input data requirements for applications on a regional scale. This implied the following simplifying assumptions:

i. The various ecosystem processes have been limited to a few key processes:
The soil solution chemistry in SMART depends solely on the net element input from the atmosphere (deposition minus net uptake minus net immobilization) and the geochemical interaction in the soil (CO_2 equilibria, weathering of carbonates, silicates and/or Al-hydroxides and cation exchange). Processes that are not taken into account, are: (i) canopy interactions, (ii) nutrient cycling processes, (iii) N fixation and NH_4^+ adsorption, (iv) uptake, immobilization and reduction of SO_4^{2-} and (v) complexation of Al^{3+} with OH^-, SO_4^{2-} and $RCOO^-$.

ii. The included processes have been represented by simplified conceptualizations: Soil interactions are either described by simple rate-limited (zero-order) reactions (e.g. uptake and silicate weathering) or by equilibrium reactions (e.g. carbonate and Al-hydroxide weathering and cation exchange). Influence of environmental factors such as pH on rate-limited reactions and rate-limitation of weathering and exchange reactions are ignored. Solute transport is described by assuming complete mixing of the element input within one homogeneous soil compartment with a constant density and a fixed depth (at least the root zone). Because SMART is a single layer soil model neglecting vertical heterogeneity, it predicts the concentration of the soil water leaving the root zone. The annual water flux percolating from this layer is taken equal to the annual precipitation, which must be specified as a model input. The time step of the model is one year, so seasonal variations are not considered. Justifications for the various assumptions and simplifications have been given by De Vries *et al.* (1989).

2.1.2 Process descriptions

An overview of the basic process descriptions used in the SMART model to predict the soil solution chemistry of soils in Europe is given in Table 2. An explanation of the symbols used is given in Annex 1.

Concentrations of SO_4^{2-} and NO_3^- are fully determined by a mass balance equation, cf Eqs. (1) and (2). For SO_4^{2-} the net input to the soil equals the SO_x deposition and for NO_3^- it equals the sum of NO_x and NH_x deposition minus uptake, immobilization and denitrification of N. The concentration of base cations in non-calcareous soils is determined by both the net input by deposition plus weathering minus uptake and a change in the adsorbed amount of base cations, Eq. (3). This change is determined by cation exchange equilibrium reactions, Eqs. (7), (8) and (9). The concentrations of HCO_3^- and Al^{3+} are determined by an equilibrium with H^+, cf Eqs. (10) and (13). The concentration of divalent base cations in calcareous soils is determined by both the net input by deposition minus uptake and a change in carbonate content, Eq. (4). In these soils carbonate weathering is included, Eq. (12), but silicate weathering, Al hydroxide weathering and cation exchange are neglected (the Al^{3+} concentration is thus set to zero). The dissociation of organic acids is modelled by Eq. (11), with a pH dependent dissociation constant (K_a). Sulphate sorption is described by a Langmuir isotherm, Eq. (6). The H^+ concentration is determined by charge balance, Eq. (14), because the model structure of SMART is based on the anion mobility concept (Reuss and Johnson, 1986). The pH is thus influenced by all rate-limited and equilibrium processes causing proton production or consumption.

Table 2 Process descriptions used in SMART to predict the soil solution chemistry (cf Posch et al., 1993)

Mass balances:

$$\frac{d}{dt}\left(\theta \cdot T_{rz} \cdot [SO_4^{2-}] + \rho_{rz} \cdot T_{rz} \cdot ctSO_{ac}\right) = SO_{4\ td} - PE \cdot [SO_4^{2-}] \quad (1)$$

$$\frac{d}{dt}\left(\theta \cdot T_{rz} \cdot [NO_3^-]\right) = N_{td} - N_{gu} - N_{im} - N_{de} - PE \cdot [NO_3^-] \quad (2)$$

BC2 in non-calcareous soils:

$$\frac{d}{dt}\left(\theta \cdot T_{rz} \cdot [BC^{2+}] + \rho_{rz} \cdot T_{rz} \cdot CEC \cdot frBC2_{ac}\right) =$$

$$BC2_{td} + BC2_{we} - BC2_{gu} - PE \cdot [BC^{2+}] \quad (3)$$

BC2 in calcareous soils:

$$\frac{d}{dt}\left(\theta \cdot T_{rz} \cdot [BC^{2+}] + \rho_{rz} \cdot T_{rz} \cdot ctBC2_{cb}\right) = BC2_{td} - BC2_{gu} - PE \cdot [BC^{2+}] \quad (4)$$

$$\frac{d}{dt}\left(\theta \cdot T_{rz} \cdot [BC^{+}]\right) = BC1_{td} + BC1_{we} + BC1_{gu} - PE \cdot [BC^{+}] \quad (5)$$

Equilibrium equations:

$$ctSO_{4\ ac} = \frac{SSC \cdot [SO_4^{2-}]}{C_{\frac{1}{2}} + [SO_4^{2-}]} \quad (6)$$

$$\frac{frH_{ac}^2}{frBC2_{ac}} = KH_{ex} \cdot \frac{[H^+]^2}{[BC^{2+}]} \quad (7)$$

$$\frac{frAl_{ac}^2}{frBC2_{ac}^3} = KAl_{ex} \cdot \frac{[Al^{3+}]^2}{[BC^{2+}]^3} \quad (8)$$

$$frH_{ac} + frBC2_{ac} + frAl_{ac} = 1 \quad (9)$$

$$[HCO_3^-] = KCO_2 \cdot \frac{pCO_2}{[H^+]} \quad (10)$$

$$[RCOO^-] = [RCOO_{tot}] \cdot \frac{K_a}{K_a + [H^+]} \quad (11)$$

$$[BC^{2+}] = \frac{KCa_{cb} \cdot pCO_2}{[HCO_3^-]^2} \quad \text{(calcareous soils only)} \quad (12)$$

$$[Al^{3+}] = KAl_{ox} \cdot [H^+]^3 \quad (13)$$

Charge balance:

$$[H^+] = [SO_4^{2-}] + [NO_3^-] + [HCO_3^-] - [Cl^-] - [BC^{2+}] - [BC^+] - [Al^{3+}] \quad (14)$$

The dissolved and adsorbed concentrations are calculated by simultaneously solving the equations in Table 2 leading to thirteen equations with thirteen unknowns, i.e. eight concentrations ($[H^+]$, $[Al^{3+}]$, $[BC^+]$, $[BC^{2+}]$, $[SO_4^{2-}]$, $[NO_3^-]$, $[HCO_3^-]$, $[RCOO^-]$), three exchangeable fractions (frH_{ac}, $frBC2_{ac}$, $frAl_{ac}$) and adsorbed SO_4^{2-} ($ctSO_{4\,ac}$). The numerical solution procedure is given in Posch *et al.* (1993).

N transformations, i.e. N immobilization, nitrification and denitrification, are described in the SMART model by rate-limited equations. The description of N immobilization is based on the assumption that the amount of organic matter (carbon) is in steady-state. Consequently, immobilization of base cations is not considered. N immobilization is described in SMART by an increase in N content in organic matter. When the C/N ratio of the soil (CN_{om}) varies between a critical and a minimum value, the immobilization rate is assumed to decrease according to:

$$N_{im} = \left(N_{td} - N_{gu} - N_{le\,mn}\right) \cdot \left(\frac{CN_{om} - CN_{mn}}{CN_{cr} - CN_{mn}}\right) \qquad \text{for } CN_{cr} > CN_{om} > CN_{mn} \qquad (15)$$

At the minimum C/N ratio (CN_{mn}), N immobilization equals zero. Above the critical value all excess nitrogen ($N_{td} - N_{gu} - N_{le\,mn}$) is assumed to immobilize. The minimum N leaching rate ($N_{le\,mn}$) is calculated by multiplying the precipitation excess by a natural background NO_3^- concentration in drainage water of 0.02 $mol_c\ m^{-3}$ (Rosén, 1990). During the simulation, the C content is fixed whereas the N content is annually updated, by adding the amount of N immobilized during each step to the N amount in the mineral topsoil. The C/N ratio is in turn updated by dividing the fixed C pool by the variable N pool according to:

$$CN_{om} = \frac{\rho_{iz} \cdot T_{iz} \cdot ctC_{iz}}{AmN_{iz}} \qquad (16)$$

Because N immobilization mainly occurs in the humus layer and the upper mineral soil (Tietema, 1992), the thickness of the zone where N immobilization (T_{iz}) occurs is taken at 20 cm.

In SMART nitrification and denitrification are described as a fraction of the net nitrate and ammonium input respectively (Posch *et al.*, 1993).

2.2 Extensions of the SMART model

Application of SMART is restricted to dry ecosystems and not suitable for calculating the N availability because it does not include a nutrient cycle. In order to model abiotic site factors in both dry and wet natural ecosystems the model must be extended with a nutrient cycle (litterfall, mineralization and uptake) and an improved modelling of hydrology, including upward and downward solute transport. In addition BC^+ must be split up in Na^+ and K^+, because K^+ is a macro nutrient whereas Na^+ is not. Most of the extensions were derived from the dynamic multi-layer model RESAM (De Vries *et al.*, 1995) and the steady-state multi-layer model MACAL (De Vries *et al.*, 1994c).

2.2.1 Mass balances

For each of the cations (Na^+, K^+, BC^{2+} (Mg^{2+}+Ca^{2+}), NH_4^+, Al^{3+}) and strong acid anions (SO_4^{2-}, NO_3^-, Cl^-) considered in SMART the mass balance equation for a compartment with depth z, is given by:

$$\frac{d}{dt}X_{tot}(z) = X_{in} + X_{int}(z) - PE(z) \cdot [X](z) + X_{sen}(z) \tag{17}$$

where X_{in} is the sum of all input fluxes to the soil. $X_{int}(z)$ is the sum of all interaction fluxes in the soil at depth z. $X_{sen}(z)$ is the net seepage flux to a soil compartment with depth z. $[X](z)$ is the concentration of ion X in the soil compartment with depth z, $mol_c\ m^{-3}$. In SMART2 the precipitation excess at depth z, $PE(z)$ is calculated as:

$$PE(z) = P \cdot (1 - f_{int}) - fr_{ru}(z) \cdot Tr \tag{18}$$

where P is the precipitation, Tr the actual transpiration, f_{int} the interception fraction (-) and $fr_{ru}(z)$ the cumulative transpiration (water uptake by roots) fraction (-) in the root zone ($z \leq T_{rz}$) at depth z, which is calculated as:

$$fr_{ru}(z) = \begin{cases} 1 - \left(\dfrac{T_{rz} - z}{T_{rz}}\right)^{ru_{exp}} & for\ z \leq T_{rz} \\ 1 & for\ z > T_{rz} \end{cases} \tag{19}$$

where T_{rz} is the thickness of the root zone (m) and ru_{exp} is an exponent determining the water uptake pattern. For $z > T_{rz}$, $fr_{ru}(z)$ equals 1, i.e. root uptake is at its maximum.

2.2.2 Seepage

Seepage is included in the mass balance, Eq. (17), as a net term, i.e. the input of upward seepage flux (X_{sen}) minus the lateral output flux (X_{la}). Figure 2 gives an overview of the water balance in the soil system including seepage. The input to the soil system consists of the throughfall flux ($P \cdot (1 - f_{int})$) and the upward seepage flux (S_e). In SMART2, upward seepage is defined as the flux at the bottom of the root zone. The upward seepage flux is assumed to be reduced at shallower depth. For the sake of simplicity for seepage the same reduction function with depth is used as for transpiration, i.e. $fr_{ru}(z)$, Eq. (19).

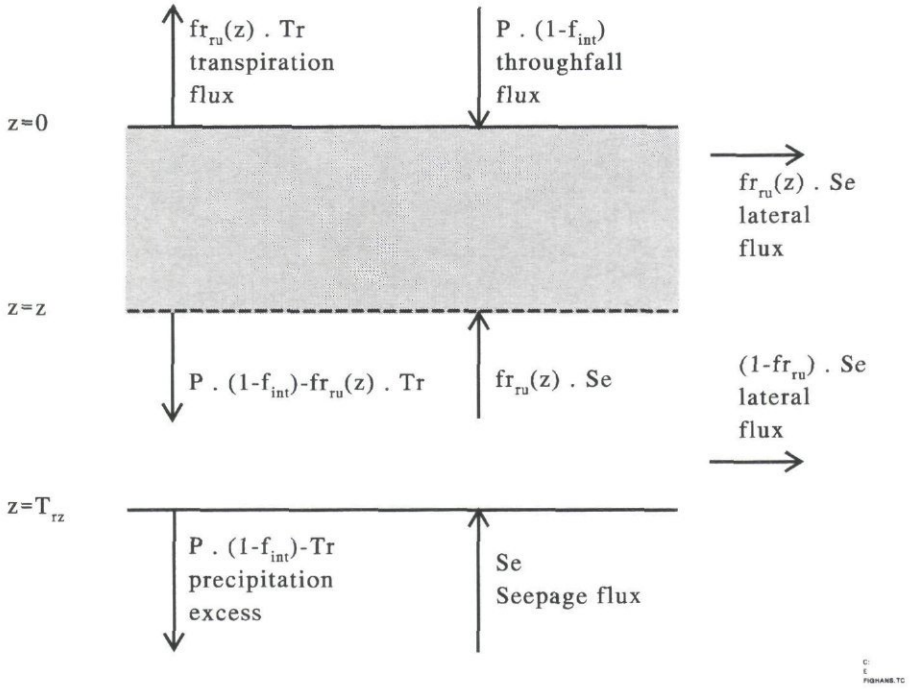

Fig. 2 Water balance in SMART2

Consequently, the seepage input to the compartment with depth z equals: $fr_{ru}(z) \cdot S_e$. The seepage flux of ion X is described as:

$$X_{se}(z) = fr_{ru}(z) \cdot [X]_{se} \cdot Se \tag{20}$$

where $[X]_{se}$ stands for the concentration of ion X in the seepage water ($mol_c\ m^{-3}$) and Se the upward seepage flux ($m\ a^{-1}$). Because it is stated that the transpiration is independent of the upward seepage flux, S_e, there must be a lateral output flux which equals the seepage input: $-fr_{ru}(z) \cdot S_e$. The concentration of ion X in the lateral output flux at depth z equals the concentration in the soil compartment, $[X](z)$. Consequently, the lateral output flux of ion X is described as:

$$X_{la}(z) = - fr_{ru}(z) \cdot [X](z) \cdot Se \tag{21}$$

where $[X](z)$ stands for the concentration of ion X in the considered soil compartment ($mol_c\ m^{-3}$) and Se the upward seepage flux ($m\ a^{-1}$). The net effect of seepage at depth z, $X_{sen}(z)$, equals $X_{se}(z) + X_{la}(z)$:

$$X_{sen}(z) = fr_{ru}(z) \cdot Se \cdot ([X_{se}] - [X](z)) \quad (22)$$

From Eq. (22) it is clear that the influence of seepage on the concentration in the considered soil compartment is larger as the concentration of ion X in the seepage water deviates more from the concentration in the soil solution. Note that the remaining part of the seepage flux that does not reach depth z is draining laterally. This lateral flux equals: $-(1 - fr_{ru}(z)) \cdot S_e \cdot [X_{se}]$.

2.2.3 Input terms

The input to the soil compartment consists of throughfall (total deposition, *td*, corrected for foliar uptake, *fu*, or foliar exudation, *fe*) and mineralization (*mi*). The input terms are described as:

$$SO_{4\,in} = SO_{4\,td} \quad (23)$$

$$NO_{3\,in} = NO_{3\,td} \quad (24)$$

$$NH_{4\,in} = NH_{4\,td} - NH_{4\,fu} + N_{mi} \quad (25)$$

$$BC2_{in} = BC2_{td} + BC2_{fe} + BC2_{mi} \quad (26)$$

$$K_{in} = K_{td} + K_{fe} + K_{mi} \quad (27)$$

$$Na_{in} = Na_{td} \quad (28)$$

2.2.3.1 Canopy interactions

The included canopy interactions in SMART2 were taken from the RESAM model (De Vries *et al.*, 1995). Foliar uptake of NH_4^+ and H^+ is described as:

$$X_{fu} = frX_{fu} \cdot X_{td} \quad (29)$$

where fX_{fu} is the foliar uptake fraction of H^+ or NH_4^+. For H_{fu} the deposition of free H^+ (H_{td}) is calculated from the charge balance:

$$H_{td} = SO_{4\,td} + NO_{3\,td} + Cl_{td} - NH_{4\,td} - BC2_{td} - K_{td} - Na_{td} \quad (30)$$

Foliar exudation of the cations (K^+, BC^{2+}) is taken equal to foliar uptake of NH_4^+ and H^+ (cf De Vries *et al.*, 1994a and b). The exudation is assumed to be triggered by exchange with these ions (Roelofs *et al.*, 1985; Ulrich, 1983). The foliar uptake of each individual cation is calculated as:

$$X_{fe} = frX_{fe} \cdot (NH_{4\,fu} + H_{fu}) \qquad X = K, BC2 \quad (31)$$

where frX_{fe} is the foliar exudation fraction of K^+ and BC^{2+} (-). The sum of fK_{fe} and $frBC2_{fe}$ equals 1.

2.2.3.2 Litterfall and root decay

The included inputs by litterfall and root decay in SMART2 affecting the mineralization flux, were also taken from the RESAM model (De Vries *et al.*, 1995). In SMART2, litterfall is the input to an organic pool containing N, BC^{2+} and K^+. Contrary to RESAM, SMART2 does not include a physical litterlayer in which a separate concentration is calculated. Only an organic pool is modelled, which has the same soil solution concentration as the mineral soil. Input fluxes of N, BC^{2+} and K^+ by litterfall, X_{lf} are described as:

$$X_{lf} = (1 - frX_{re}) \cdot Am_{lf} \cdot ctX_{lv} \tag{32}$$

where Am_{lf} is the amount of litterfall (kg ha^{-1} a^{-1}), ctX_{lv} is the contents of element X in leaves (mol_c kg^{-1}) and frX_{re} are reallocation fractions for element X in leaves (-). Reallocation of K^+ and BC^{2+} in leaves prior to litterfall is considered negligible (i.e. $frK_{re} = frBC2_{re} = 0$). The actual amount of litterfall is linearly related to the actual amount of stems (cf section 2.2.4.1)

High contents of N in leaves and fine roots in Dutch forests are caused by the high N deposition level. To account for this effect, the N content in leaves is calculated as a function of the N deposition according to:

$$ctN_{lv} = ctN_{lv\ mn} + (ctN_{lv\ mx} - ctN_{lv\ mn}) \cdot \left(\frac{N_{td} - N_{td\ mn}}{N_{td\ mx} - N_{td\ mn}} \right) \tag{33}$$

$$\text{for } N_{td\ mn} < N_{td} < N_{td\ mx}$$

where $ctN_{lv\ mn}$ and $ctN_{lv\ mx}$ are the minimum and maximum N content in leaves (mol_c kg^{-1}) and $N_{td\ mn}$ and $N_{td\ mx}$ are the minimum and maximum total deposition levels of N (mol_c ha^{-1} a^{-1}) between which the N content of leaves is influenced. When N_{dt} is less than $N_{td\ mn}$, $ctN_{lv} = ctN_{lv\ mn}$ and when N_{td} is greater than $N_{td\ mx}$, $ctN_{lv} = ctN_{lv\ mx}$. For the Netherlands $N_{td\ mn}$ = 1500 $kmol_c$ ha^{-1} a^{-1} and $N_{td\ mn}$ = 7000 $kmol_c$ ha^{-1} a^{-1} were used. Contrary to RESAM the reallocation fraction (frX_{re}) is not considered as a function of the N content in the foliage, frX_{re} remains constant during the simulation period.

The dynamic turnover of fine roots is coupled with the amount of litterfall and split up between the litter compartment (depth independent) and the mineral soil (depth dependent). The root decay flux in the litter compartment ($X_{rd\ lt}$) is described as:

$$X_{rd\ lt} = X_{lf} \cdot ncf \cdot fr_{rt\ lt} \tag{34}$$

where ncf is the nutrient cycling factor (-), which is defined as the ratio of the above ground nitrogen cycle (litterfall flux) and the root turnover (related to nitrogen), and $fr_{rt\ lt}$ is the fraction of fine roots in the litter layer (-). The depth-dependent root decay flux in the mineral soil ($X_{rd\ ms}$ (z)) is described as:

$$X_{rd\ ms}(z) = fr_{ru}(z) \cdot X_{lf} \cdot ncf \cdot (1 - fr_{rt\ lt}) \quad (35)$$

2.2.3.3 Mineralization

As with canopy interactions, litterfall and root decay, mineralization in SMART2 is also taken from the RESAM model. For the simulation of the decomposition of above-ground organic matter (litter including dead roots in the litter layer) a distinction is made between a rapidly decomposing pool of fresh litter (less than one year old) and a slowly decomposing pool of old litter (more than one year) (Janssen, 1984). The mineralization flux of N (during mineralization, N is released as NH_4^+), K^+ and BC^{2+} ($mol_c\ ha^{-1}\ a^{-1}$) from fresh litter, $X_{mi\ fl}$, is described as a fraction of the input of X by litterfall and root decay in the litter compartment according to:

$$X_{mi\ fl} = \left(frX_{le} + fr_{mi} \cdot (1 - frX_{le})\right) \cdot X_{lf} \cdot (1 + ncf \cdot fr_{rt\ lt}) \quad (36)$$

where fr_{mi} is a mineralization fraction (-) and frX_{le} is a leaching fraction (-). Leaching only refers to the release of BC^{2+} (Ca^{2+} and Mg^{2+}) and K^+ from fresh litter just after litterfall, a process which is especially important for K^+. Actually, leaching is a process which differs from mineralization because organic matter is not decomposed.

Fresh litter which is not mineralized is transferred to the old litter (humus) pool. The mineralization flux of NH_4^+, K^+ and BC^{2+} from this litter pool, $X_{mi\ lt}$, is described by first-order kinetics (Van Veen, 1977):

$$X_{mi\ lt} = k_{mi\ lt} \cdot Am_{lt} \cdot ctX_{lt} \quad (37)$$

where $k_{mi\ lt}$ is the mineralization rate constant from old litter (a^{-1}), Am_{lt} is the amount of old litter ($kg\ ha^{-1}$) and ctX_{lt} is the content of element X in old litter ($mol_c\ kg^{-1}$). At present, mineralization of organic matter in the mineral soil layers is not considered in SMART2, except for the mineralization from root necro-mass, which is fed by root decay as described before. Root decay in the mineral soil is considered to be mineralized completely. The total mineralization flux at depth z becomes equal to:

$$X_{mi}(z) = X_{mi\ lt} + X_{mi\ fl} + X_{rd\ ms}(z) \quad (38)$$

The flux of organic anions, $RCOO_{mi}$, produced during mineralization from both fresh and old litter and from dead root ($mol_c\ ha^{-1}\ a^{-1}$) is calculated from charge balance considerations:

$$RCOO_{mi} = N_{mi} + Ca_{mi} + Mg_{mi} + K_{mi} - SO_{4\ mi} \quad (39)$$

Actual values for the mineralization fraction, $fr_{mi\ fl/lt}$, and mineralization rate constant, $k_{mi\ fl/lt}$, are described in SMART2 as maximum values, which are reduced for

environmental factors such as soil moisture (water-table), pH and the C/N ratio. For all constituents the maximum value ($k/f_{mi\ mx}$) is influenced by the mean water-table during spring time (Mean Spring Water-table, *MSW*) and the pH. The N mineralization is also influenced by the C/N ratio:

$$k/fr_{mi} = k/fr_{mi\ mx} \cdot rf_{mi\ GVG} \cdot rf_{mi\ pH} \cdot rf_{mi\ CN} \tag{40}$$

where $rf_{mi\ MSW}$, $rf_{mi\ pH}$ and $rf_{mi\ CN}$ are the reduction factors for water-table, pH and N content (C/N ratio) respectively (-). For BC^{2+} and K^+ $rf_{mi\ CN}$ is always 1. The reduction functions for water-table and pH were taken from RESAM (cf Kros *et al.*, in prep.):

$$rf_{mi\ GT} = \begin{cases} 0.25 & \text{for } MSW < 0.45 \\ log10\ (8 \cdot MSW) & \text{for } 0.45 \leq MSW \leq 1.25 \\ 1 & \text{for } MSW > 1.25 \end{cases} \tag{41}$$

$$rf_{mi\ pH} = \begin{cases} 0 & \text{for } pH<2.5 \\ \dfrac{pH - 2.5}{2} & \text{for } 2.5 \leq pH < 3.5 \\ \dfrac{pH - 1}{5} & \text{for } 3.5 \leq pH \leq 6 \\ 1 & \text{for } pH>6 \end{cases} \tag{42}$$

The N mineralization values are reduced at low N contents (high C/N ratios) to account for immobilization by microbes according to (Janssen, 1983):

$$rf_{mi\ CN} = 1 - \frac{\dfrac{ctC_s}{ctN_s} - CN_{mo}}{DA_{mo} \cdot CN_{mo}} \quad \text{for } CN_{mo} < \frac{ctC_s}{ctN_s} < (1+DA_{mo}) \cdot CN_{mo} \tag{43}$$

where CN_{mo} is the C/N ratio of the micro-organisms decomposing the substrate (-), ctC_s/ctN_s is the C/N ratio of the substrate (fresh litter (*s=fl*), old litter (*s=lt*)) and DA_{mo} is the dissimilation to assimilation ratio of the decomposing microbes (-). If ctC_s/ctN_s is less then CN_{mo}, $rf_{mi\ CN} = 1$ and if CN_{mo} is more than $(1+DA_{mo}) \cdot CN_{mo}$, $rf_{mi\ CN} = 0$. Values for DA_{mo} and CN_{mo} are related to fungi because they are mainly responsible for mineralization of forest litter.

2.2.4 Interaction terms

The interaction fluxes for NH_4^+, NO_3^-, BC^{2+} and K^+ accounted for in SMART2 are base cation weathering, root uptake, nitrification and denitrification. In comparison with SMART these terms are extended with nutrient maintenance uptake, and extended with reduction functions for nitrification and denitrification as a function of pH and groundwater level (cf section 2.2.4.2). Furthermore, interaction fluxes at depth z are described as functions with depth (z), according to:

$$SO_{4\ int}(z) = 0 \tag{44}$$

$$NO_{3\ int}(z) = fr_{ru}(z) \cdot (NH_{4\ ni} - NO_{3\ ru} - NO_{3\ de}) \tag{45}$$

$$NH_{4\ int}(z) = - fr_{ru}(z) \cdot (NH_{4\ ni} + NH_{4\ ru}) \tag{46}$$

$$BC2_{int}(z) = - fr_{ru}(z) \cdot BC2_{ru} + BC2_{we} \cdot z \tag{47}$$

$$K_{int}(z) = - fr_{ru}(z) \cdot K_{ru} + K_{we} \cdot z \tag{48}$$

$$Na_{int}(z) = Na_{we} \cdot z \tag{49}$$

where the subscript *we* stands for weathering, *ru* for root uptake, *ni* for nitrification and *de* for denitrification.

2.2.4.1 Nutrient uptake

Nutrient uptake is treated in the same way as it was done in the MACAL model (De Vries *et al.*, 1994c). Total root uptake of NH_4^+, NO_3^-, BC^{2+} (Ca^{2+}, Mg^{2+}), K^+ is described in SMART2 as a demand function, which consists of maintenance uptake, to resupply the needles/leaves/shoots and roots (steady-state situation), and net (growth) uptake in stems and branches. The total root uptake fluxes for NH_4^+, NO_3^-, BC^{2+} and K^+ ($mol_c\ ha^{-1}\ a^{-1}$) are thus described as:

$$NO_{3\ ru} = \left(N_{lf} - N_{fu} + N_{gu}\right) \cdot \frac{NO_{3\ in}}{N_{in}} \tag{50}$$

$$NH_{4\ ru} = \left(N_{lf} - N_{fu} + N_{gu}\right) \cdot \frac{NH_{4\ in}}{N_{in}} \tag{51}$$

$$BC2_{ru} = BC2_{lf} + BC2_{fe} + BC2_{gu} \tag{52}$$

$$K_{ru} = K_{lf} + K_{fe} + K_{gu} \tag{53}$$

where *gu* stands for growth uptake, and N for NH_4^+ plus NO_3^-.

Growth uptake by stems and branches is forced by a logistic growth function:

$$Am_{st}(t) = \frac{Am_{st\ mx}}{(1 + \exp(-k_{gl} \cdot (age_{vg} + t - t_{\frac{1}{2}}))} \quad (54)$$

where $Am_{st}(t)$ is the amount of stems (and branches) for year = t (kg ha^{-1}), $Am_{st\ mx}$ the maximum amount of stems (kg ha^{-1}), age_{vg} the initial age of the vegetation (forest), $t_{½}$ half life-time (a), k_{gl} is the logistic growth rate constant (kg ha^{-1} a^{-1}).

The growth uptake is then calculated as:

$$X_{gu} = (Am_{st}(t) - Am_{st}(t-1)) \cdot ctX_{sh} \quad (55)$$

where $(Am_{st}(t) - Am_{st}(t-1))$ is the increment in amount stems for the current year (=time step) (kg ha^{-1} a^{-1}) and ctX_{st} is the content of element X in stems (mol$_c$ kg^{-1}).

In the model the amount of litterfall (Am_{lf}, cf section 2.2.3.2) is linked to the amount of stems according to:

$$Am_{lf} = Am_{lf\ mx} \cdot \frac{Am_{st}}{Am_{st\ mx}} \quad (56)$$

where $Am_{lf\ mx}$ is the maximum amount of litterfall (kg ha^{-1} a^{-1}). In practice, however, for an average forest the maximum amount of litterfall is established several decades earlier than the maximum amount of stems.

2.2.4.2 Nitrification and denitrification

Nitrification and denitrification for the complete soil layer (mol$_c$ ha^{-1} a^{-1}) are described in SMART2 as a fraction of the net input:

$$NH_{4\ ni} = fr_{ni} \cdot (NH_{4\ in} - NH_{4\ ru} - NH_{4\ im} + NH_{4\ mi}) \quad (57)$$

$$NO_{3\ de} = fr_{de} \cdot (NO_{3\ in} - NO_{3\ ru} - NO_{3\ im} + NH_{4\ ni}) \quad (58)$$

where fr_{ni} and fr_{de} are the nitrification and denitrification fractions (-), $NH_{4\ in}$ and $NO_{3\ in}$ stand for the gross input fluxes of NH_4^+ and NO_3^-, respectively, cf Eqs. (25) and (24), $NH_{4\ ru}$ and $NO_{3\ ru}$ stands for the root uptake fluxes of NH_4^+ and NO_3^- respectively, cf Eqs. (51) and (50), $NH_{4\ im}$ and $NO_{3\ im}$ stands for the immobilization fluxes in the mineral soil of NH_4^+ and NO_3^- respectively, Eq. (15) (cf De Vries *et al.*, 1994d). As with mineralization, the maximum values for the nitrification and denitrification rate constant, $fr_{ni\ mx}$ and $fr_{de\ mx}$, are adjusted by the mean water-table and pH:

$$fr_{ni} = fr_{ni\ mx} \cdot rf_{ni\ MSW} \cdot rf_{ni\ pH} \tag{59}$$

$$fr_{de} = fr_{de\ mx} \cdot rf_{de\ GVG} \cdot rf_{de\ pH} \tag{60}$$

where $rf_{ni/de\ MSW}$ and $rf_{ni/de\ pH}$ are the nitrification and the denitrification reduction factors for the water-table and pH respectively (-). Maximum values are reduced with a decreasing mean spring water-table for nitrification, because this process is restricted to aerobic conditions, whereas the opposite is true for denitrification. Both rate constants are also reduced with decreasing pH.

The nitrification reduction functions for mean spring water-table is described as:

$$rf_{ni\ MSW} = \begin{cases} rf_{ni\ MSW\ mn} & \text{for } MSW < z1 \\ a_{ni} + b_{ni} \cdot MSW & \text{for } z1 \leq MSW < z2 \\ 1 & \text{for } MSW \geq z2 \end{cases} \tag{61}$$

were $rfr_{ni\ MSW\ mn}$ is the soil dependent minimum value of the reduction function (-), a_{ni} (-) and b_{ni} (m^{-1}) are soil dependent parameters, and $z1$ and $z2$ are soil dependent MSW (m) values where the reduction function is changed.

The nitrification reduction function for pH is described as (cf Kros *et al.*, in prep.):

$$rf_{ni\ pH} = \frac{1}{1 + e^{4 \cdot (3.75 - pH)}} \tag{62}$$

The denitrification reduction function for mean spring water-table is described as:

$$rf_{de\ MSW} = \begin{cases} 1 - a_{de} \cdot MSW & \text{for } MSW \leq 1.5\ m \\ rf_{de\ MSW\ mn} & \text{for } MSW > 1.5\ m \end{cases} \tag{63}$$

where a_{de} (m^{-1}) is a soil-dependent parameter and $rf_{de\ MSW\ mn}$ (-) the soil-dependent minimum value for $rf_{de\ MSW}$.

The denitrification reduction function for mean pH is described as (cf Kros *et al.*, in prep.):

$$rf_{de\ pH} = \begin{cases} 0 & \text{for } pH < 3.5 \\ \dfrac{pH - 3.5}{3} & \text{for } 3.5 \leq pH < 6.5 \\ 1 & \text{for } pH \geq 6.5 \end{cases} \tag{64}$$

2.3 The MOVE model

The vegetation module predicts the probability of species occurrence as a function of three abiotic soil factors: soil acidity, nutrient availability and soil moisture. With regression statistics the occurrence probability of a species can be calculated for each combination of soil factors or for each environmental variable separately resulting in species-response curves. Species-response curves of 700 plant species have been determined for soil moisture, nutrient availability and soil acidity (Wiertz *et al.*, 1992) using Gaussian logistic regression models.

Regression was based on an extensive database developed for a revision of the Dutch classification of plant communities (Schaminee *et al.*, 1989). This database consists of 17 000 vegetation relevés. No information on abiotic site factors of the vegetation relevés was available. These were assessed in retrospect with Ellenberg indication values (Ellenberg *et al.*, 1991), using the method of Ter Braak and Gremmen (1987). Ellenberg indication values indicate the relationship between the occurrence of plant species and nutrient availability, acidity, soil moisture, salt dependency, and temperature. These values have been assigned to most plant species of western and central Europe, and the Netherlands (Wiertz *et al.*, 1992). The abiotic site factors of each vegetation relevé are assessed by averaging the indication values of all the species recorded. Calculated averages, in Ellenberg indication values, are used as a semi-quantitative assessment of the abiotic soil factors. Next, the occurrence frequency of each species is established as a function of the averages of vegetation relevés. The occurrence frequency is described with Gaussian logistic regression models (Jongman *et al.*, 1987). Since this analysis uses floristic information to assess the abiotic site factors, any (historical) vegetation sample can be included in the analysis, extending the database. Moreover, such an analysis excludes potential bias caused by high temporal and spatial variation in the actual measurements of abiotic site factors. Deducing values for the abiotic soil factors from the vegetation sample guarantees ecological relevance.

Species occurrence has been described as being significant for 95% of the species using unimodal and linear regression models. Most of the significant models were unimodal. Linear models were found for nutrients (4%) and salt (20%).

Ellenberg indication values can be calibrated with quantitative values for the abiotic soil factors using combined samples of vegetation and environmental variables. This calibration connects SMART2 with MOVE. For this purpose a database has been compiled with combined samples for pH (N = 3988), *MSW* (N = 13) and N production (N = 266). For pH, *MSW*, biomass production and N production satisfying relations with Ellenberg values were found, explained variances of respectively 0.58, 0.54, 0.59 and 0.58 (Alkemade *et al.*, 1996)

2.3.1 MOVE input

For the time being the MOVE input consist of a yearly average pH and N availability in the root zone and the mean spring watertable (*MSW*). The pH and N availability are calculated by SMART2 (cf section 2.2) whereas the *MSW* is derived from the output from the LGM model (cf section 3.3.2.1). The pH refers to a 'real' pH of the soil solution, which must not be mixed up with regular soil analysis parameters like pH(KCl) and pH(H_2O). In this study the N availability is defined as the sum of the N throughfall flux and the mineralization flux. This can be regarded as a gross N availability, which is available for root uptake, immobilization and denitrification. The remainder will be leached from the root zone.

3 Application methodology and input data

3.1 Data acquisition strategy

For application of SMART2 on a national scale, data were needed with respect to system inputs (driving variables), the initial state of model variables and model parameters. Model inputs refer to a specific deposition scenario and seepage scenario for each grid cell, whereas the model variables and parameters refer to distinguished combinations of generic soil types and generic vegetation types.

In predicting of the long-term impact of atmospheric deposition and seepage on site factors on a national scale, a distinction was made in:
- geo-referenced information on model inputs, varying between each grid cell considered, i.e. (i) the area of vegetation soil combinations (a multiple of 0.625 km^2 cf Section 3.3), (ii) the deposition of SO_4^{2-}, NO_3^-, NH_4^+, base cations and Cl^- (iii) precipitation and (iv) seepage fluxes;
- generic information, i.e. average values for initial values of model variables and model parameters for each combination of vegetation type and soil type.

Hydrological information was derived from the National Groundwater Model (LGM; Pastoors, 1993), with a resolution of 1 x 1 km^2. All other geographical information was transformed to, a 1 x 1 km^2 grid, because of portability reasons towards the LGM model and the National Survey on Landscape Ecology (LKN; Klijn, 1989). This refers to deposition values of SO_2, NO_x and NH_3 for 1990 (derived from a 5 x 5 km^2 grid database; Erisman, 1991) and deposition values of base cations and Cl^- (derived from a 10 x 10 km^2 grid database; De Vries *et al.*, 1994c). The grid related information was stored in database tables (using ORACLE at SC-DLO and INGRES at RIVM), whereas the vegetation and soil related parameter were stored in ASCII files. The model output was stored as grid and time related data in database tables. The data model showing all tables is provided in Figure 3.

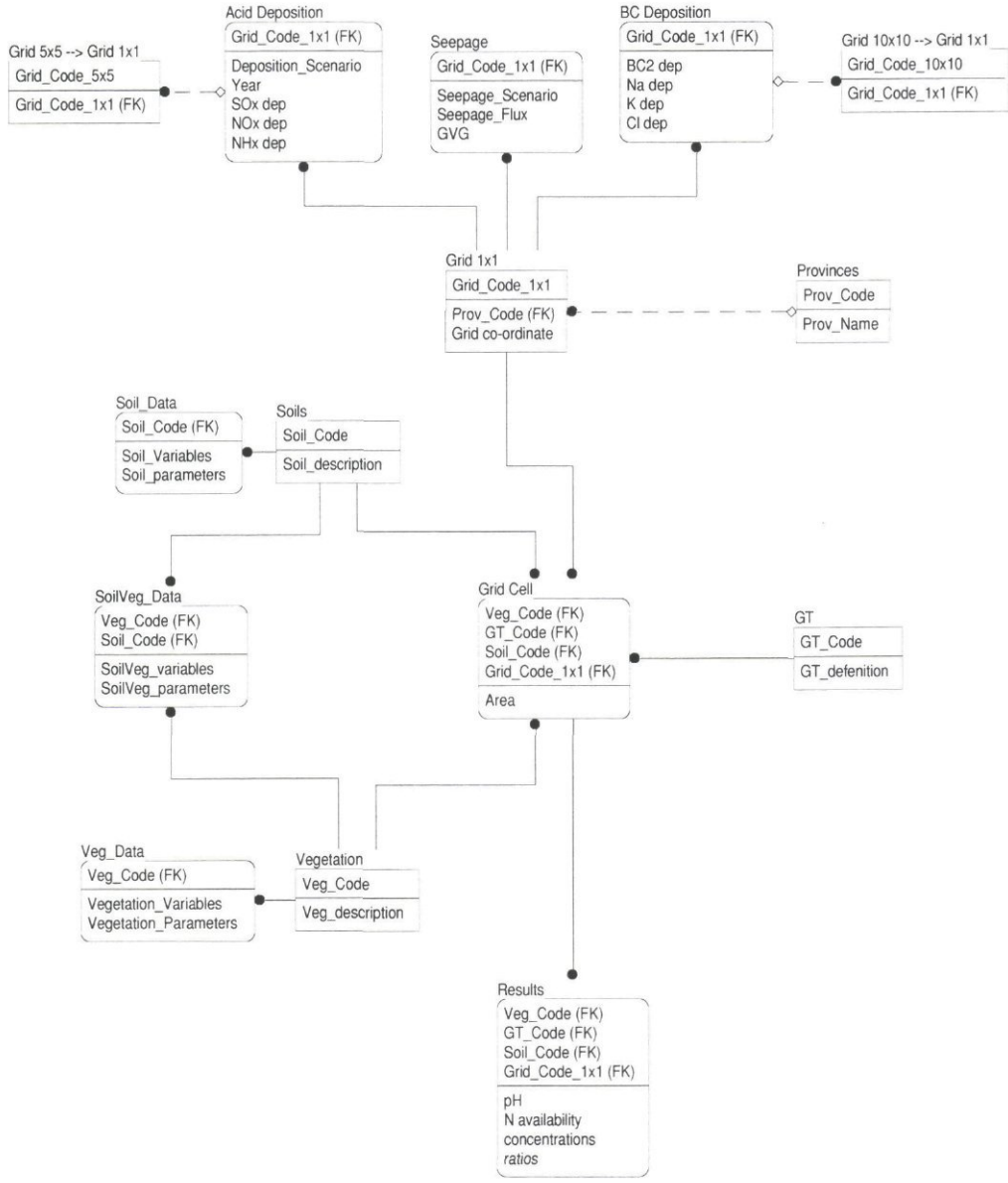

Fig. 3 Data model for the national application of SMART2

3.2 Areal distribution of soil-vegetation combinations

A distinction was made in seven soil types and five water-table classes, which were derived from the 1 : 50 000 soil map of the Netherlands. The generalization of soil types was based on soil chemical criteria: parent material, presence of calcite, base saturation and texture (Table 3).

Table 3 Distinguished soil types

Code	Soil class	Common soil types (FAO, 1988)
SP	Sand Poor	Carbic Podzols, Arenosols
SR	Sand Rich	Gleyic Podzols, Gleysols
SC	Sand Calcareous	Arenosols
CN	Clay Non-calcareous	Fluvisols
CC	Clay Calcareous	Fluvisols
PN	Peat Non-calcareous	Histosols
LN	Loess Non-calcareous	Luvisols

The relation between the 1 : 50 000 soil map codes and the seven soil types used is given in Annex 3. The five water-table classes were the same as used by De Waal (1992) (Table 4). The corresponding Mean Highest Water-table (*MHW*) and Mean Lowest Water-table (*MLW*) were derived (weighted averaged) from Van der Sluijs (1990).

Table 4 Used water-table classes and their corresponding water-table classes from the 1 : 50 000 soil map of the Netherlands and the corresponding averaged MHW and MLW

Water-table Class used in this study	Water-table Class from the 1 : 50 0000 soil map	*MHW*[1)] (m)	*MLW* (m)
1	I	-0.05	0.38
2	II	0.07	0.66
3	II*, III, III*, V, V*	0.24	1.18
4	IV, VI	0.60	1.43
5	VII, VII*	1.29	2.21

[1)] Averaged *MHW* and *MLW* as given by Van de Sluijs (1990)

The considered vegetation structures were lumped into five vegetation types (Table 5). The generalization of vegetation was based on difference in canopy characteristics, litter production, growth and vegetation management.

The areal distribution of the vegetation types over the soil types (Table 6) and over the water-table classes (Table 7) was obtained by an overlay of 250 x 250 m^2 grid maps, i.e. (i) generalized soil map (including water-table information), (ii) the Dutch forest inventory (Nederlandse, 1985), (iii) 'nature value map' (Natuurbeleidsplan, 1989) and a detailed vegetation map based on satellite observations (LGN; Thunnissen *et al.*, 1992). Because of the inaccuracy of the various vegetation maps, more than one vegetation class could be assigned to a 250 x 250 m^2 grid cell. For these cases the following allocation sequence was used: (i) grassland and heather from the satellite observation map was first assigned to the 250 x 250 m^2 grid cells; (ii) forest (DEC, SPR, PIN) was only assigned when no grassland and no heather was assigned during the previous step.

Table 5 Distinguished vegetation classes

Code	Vegetation Class	Common species Characteristics
DEC	Deciduous forest	Oak, beech, Japanese larch Needle or leave sheddy trees with: low forest filtering, growth rate and transpiration rate
PIN	Pine forest	Scots pine and black pine Evergreen trees with: moderate forest filtering, growth rate and transpiration rate
SPR	Spruce forest	Douglas fir, Norway spruce Evergreen trees with: high forest filtering, growth rate and transpiration rate
HEA	Heather	Calluna, Erica
GRP	(nutrient-poor) Grassland	Common grass species no fertilization or grazing

Table 6 Area of the vegetation/soil combinations considered in the model application as a percentage of the total vegetation-covered area in the Netherlands[1] (326 614 ha)[2]

Soil type	Area (%)					
	Pine forest	Spruce Forest	Deciduous forest	Heather	Grass (nutrient-) Poor	Total
Sand Poor	35.54	5.97	18.73	3.70	3.19	67.14
Sand Rich	4.97	3.11	10.19	0.18	0.29	18.74
Sand Calcareous	0.29	0.12	1.28	0.00	2.94	4.63
Clay Non-calcareous	0.27	0.30	2.57	0.00	0.27	3.42
Clay Calcareous	0.02	0.03	2.21	0.00	0.29	2.54
Peat Non-calcareous	0.22	0.39	1.62	0.12	0.44	2.79
Loess Non-calcareous	0.14	0.05	0.52	0.02	0.02	0.74
Total	41.45	9.97	37.12	4.02	7.44	100.00

1) Information on the areal distribution of tree species and soil types in each grid cell was derived by overlaying a 250 x 250 m^2 grid with vegetation coverage information and a soil database with soil type information in a 250 x 250 m^2 grid. The latter database was derived by transforming the digitized 1 : 50 000 soil polygon map of the Netherlands (De Vries and Denneboom, 1992).

2) This value excludes the vegetation coverage in the southern part of the Province of Limburg and the southern part of the Province of Flevoland.

Table 7 Area of the vegetation/water-table class combinations considered in the model application as a percentage of the total vegetation covered area in the Netherlands (326 614 ha)

Water-table Class	Area (%)					
	Pine forest	Spruce Forest	Deciduous forest	Heather	Grass (nutrient-) Poor	Total
1	0.03	0.01	0.28	0.01	0.50	0.82
2	0.21	0.13	1.25	0.01	0.99	2.59
3	5.66	3.41	11.75	0.61	1.21	22.64
4	5.77	2.72	8.81	0.22	1.08	18.60
5	29.76	3.71	15.02	3.18	3.67	55.35
Total	41.43	9.98	37.11	4.03	7.45	100.00

3.3 Deposition and seepage scenarios

The temporal trends of chemical soil parameters (a.o. the site factors) predicted by SMART2 are driven by scenarios for quantity and quality of the atmospheric deposition, seepage and related changes in phreatic water level. The scenarios considered only related to the quality of atmospheric deposition and the quantity of seepage (cf Table 8).

Table 8 Considered scenarios with respect to quality and quantity

Aspect	Deposition	Seepage
Quantity	Constant[1)]	Variable
Quality	Variable[2)]	Constant

1) Refers to precipitation

2) Refers to SO_x, NO_x and NH_3. Atmospheric deposition of base cations and chloride was assumed to be constant

3.3.1 Deposition scenarios

Initial deposition estimates for NH_x, NO_x and SO_x were taken from Erisman (1991). Erisman developed an empirical model (DEADM) for the calculation of the wet and dry deposition of these elements on a national scale for a 5 x 5 km^2 grid, using the concentrations of NH_x, NO_x and SO_x that were measured at several weather stations of the National Air Quality Monitoring Network. For each 1 x 1 km^2 values from the corresponding 5 x 5 km^2 grid were used.

Two deposition scenarios were generated: (i) a constant deposition scenario and (ii) a reducing deposition scenario, reflecting the planned emission reductions in the Netherlands. Values for each grid between 1990 and 2050 were derived by linear interpolation, using the initial deposition estimates for 1990 (cf Section 3.3.1) and the reductions factors from Table 9.

Table 9 Reduction factors for NH_x, NO_x and SO_x in each grid and the corresponding average deposition for the Reducing Deposition Scenario

Period	Reduction factors[2] (-)			Deposition[2] (mol_c ha^{-1} a^{-1})		
	NH_x	NO_x	SO_x	NH_x	NO_x	SO_x
1990-2000	0.52	0.74	0.65	2150	950	1300
2000-2010	0.40	0.62	0.42	1100	700	840
2010-2050	0.40	0.62	0.42	850	590	540

[1] Reduction factors are related to the deposition in 1990
[2] Deposition values refer to the beginning year of the period

Values used for the deposition of base cations and Cl^- were taken from De Vries (1991), who performed an interpolation from 22 monitoring-stations for the period 1978-1985 (Chemische, 1985) to a 10 x 10 km^2 grid. For each 1 x 1 km^2 grid values from the corresponding 10 x 10 km^2 grid were used. Base cation and Cl^- deposition fluxes were kept constant throughout the simulation period.

Precipitation data were derived from weather stations from the Royal Netherlands Meteorological Institute (KNMI). Selected records of precipitation normals from 280 stations over the period 1950-1980 were interpolated to a 10 x 10 km^2 grid. As with the base cation deposition, values for each 1 x 1 km^2 cell were taken from the corresponding 10 x 10 km^2 grid and were assumed constant during the simulation period (cf Table 8). Details on the interpolation procedure have been given in Hootsmans and Van Uffelen (1991, internal report). Most values ranged between 700 and 900 mm a^{-1}.

3.3.2 Seepage scenarios

3.3.2.1 Seepage quantity

Scenarios for the quantity of seepage were generated with the National Groundwater Model for the Netherlands (LGM, Pastoors, 1993). The LGM was developed and used for the National Policy Plan on Drinking Water and Industrial Water Supply to assess the effect of changes in groundwater abstractions on the geo-hydrological system. These effects are expressed in terms of hydrological variables: changes in phreatic water level, groundwater heads in deeper aquifers, fluxes between the upper boundary of the geo-hydrological system and the first aquifer, and fluxes across the aquitard.

The effects of seepage on the site factors were evaluated for two scenarios: (i) a constant seepage flux, using the values for the year 1988 as presented by Pastoors (1993), and (ii) the MER/DIV scenario, i.e. 25% reduction of groundwater abstractions for public drinking water (cf Pastoors, 1992), resulting in increased seepage fluxes for the year 2010. For the second scenario, values between 1988 and 2010 were linearly interpolated. It must be emphasised that the used hydrological scenario only influenced a relative small part of the country. Consequently, the

expected effects on a national scale will be small. The surface area that showed an increase in seepage flux is restricted to about 12% of the model area, which is only 9% of the surface area of the Netherlands (cf Pastoors, 1992).

The changes in phreatic water level were derived from the groundwater heads in the first aquifer, using (cf Pastoors, 1993):

$$\Delta\varphi_{0,i} = \Delta\varphi_{1,i} \cdot \frac{\gamma}{(\gamma + c_{0,i})} \tag{65}$$

where:

$\Delta\varphi_{0,i}$ = change in phreatic water level in grid i (m)
$\Delta\varphi_{1,i}$ = change in ground water head of the first aquifer in grid i (m)
γ = drainage resistance (d)
$c_{0,i}$ = resistance of top-layer in grid i (d)

Values used for the resistance of the top layer, which are related to the water-table classes used, are given in Table 10. Data were derived from Pastoors (1993).

The changes in phreatic water were converted to absolute values by adding them to the initial phreatic ground water level:

$$MSW = MSW_0 - \Delta\varphi_0 \tag{66}$$

where:
MSW = Actual Mean Spring Water-table (m)
MSW_0 = Initial Mean Spring Water-table (m)

MSW_0 is calculated from the mean highest water-table (MHW) and the mean lowest water-table (MLW) as given in Table 4, according to Van der Sluijs (1990):

$$MSW_0 = 0.054 + 0.83 \cdot MLW + 0.19 \cdot MLW \tag{67}$$

Unfortunately, the LGM calculates only one value per 1 km^2 grid cell, which refers to the dominant water-table class. In order to make also calculations for other water-table classes in the considered grid cell, it was decided to assign the calculated seepage flux only to the dominant water-table class and lower classes (cf Section 3.2). For higher water-table classes a seepage flux of zero was assumed. Furthermore, the LGM model covers only 75% of the surface area of the Netherlands. Because of the presence of brackish and saline groundwater in the western and northern part of the country was not covered by LGM, see Annex 2. In addition, also some areas in the southern part and the eastern part were excluded.

Table 10 Drainage resistance, γ (d) used for the distinguished water-table classes

Water-table Class	γ (d)
1	100
2	150
3	300
4	400
5	700

For the area that was not covered by the LGM model the seepage flux was assumed to be zero. However, for large parts of the western part of the Netherlands this is not true. One should be aware of this shortage when regarding the results.

3.3.2.2 Seepage quality

Information on seepage water chemistry was based on the National Survey on landscape ecology (LKN; Bolsius, *et al.*, 1994). For each 1 km^2 grid cell, the LKN groundwater quality database provides a quality class (Table 11).

Table 11 Seepage quality classes as used in the LKN groundwater quality database and the (mixture of) water type(s) used for the derivation of the concentration

LKN type	Description	Reference water type
0	no seepage	this type is set equal to type 1 when LGM calculates seepage for these grid cells
1	mixed water	50% LI-ANG + 50% AT-W80
2	groundwater	LI-ANG
3	brackish water	10% TH-N70 + 90% AT-W80
4	sea water	TH-N70

In order to assign a chemical composition to the quality classes, the chemical composition of reference water types from Van Wirdum (1991) were used. Van Wirdum (1991) introduced 3 reference types:

- lithotrophic type, a relatively Ca-rich groundwater, sampled at Angeren (Province of Gelderland), 24 m below soil surface on December 8, 1980: LI-ANG;
- atmotrophic type, relatively unpolluted precipitation, the weighted mean composition of rain water collected at Witteveen (Province of Drenthe), during 1980: AT-W80;
- thalassotrophic type, water from the North Sea, sampled at 70 km from the coast at Noordwijk on July, 27, 1982: TH-N70.

Using the chemical concentrations of the reference samples from Van Wirdum (1991) and the assumed mixtures (cf Table 11), ionic concentrations were derived for LKN groundwater quality types (Table 12).

Table 12 Groundwater concentrations ($mol_c\ m^{-3}$) used for the LKN type

LKN type	SO_4^{2-}	NO_3^-	NH_4^+	BC^{2+} [1)]	K^+	Na^+	Cl^-
0	0.20	0.06	0.05	3.23	0.03	0.30	0.20
1	0.20	0.06	0.05	3.23	0.03	0.30	0.20
2	0.27	0.02	0.04	6.42	0.05	0.52	0.31
3	5.74	0.02	0.12	19.5	1.05	46.0	54.1
4	55.0	0.02	0.78	137.7	10.0	456.0	538.0

[1)] $BC^{2+} = Ca^{2+} + Mg^{2+}$

3.4 Data related to vegetation types

Data used for the five vegetation types are presented in Table 13. The vegetation age (age_{vg}) was set to 40 years old for forest and 10 years old for short vegetation. This refers to a semi mature forest which will double in biomass during the next 50 years. The stand age (age_{lt}) for forest (PIN, SPR, DEC) was derived by assuming that most of the actual forest in the Netherlands was planted at the beginning of the 20^{th} century. For heather (HEA) and grassland (GRP) is was assumed that they were sod cutted or ploughed 10 years ago.

Most data related to canopy interactions (filtering factors, dry deposition factors, interception fractions, foliar uptake fractions and foliar exudation fractions), nutrient cycling (reallocation fractions and nutrient contents in leaves) and growth uptake (nutrient contents in stems) for forests were directly taken form De Vries *et al.* (1994c). Values for pine, spruce and deciduous were related to Scots pine, Douglas fir and Oak respectively. The amounts of litterfall for these forests were the product of the average values for leaf biomass and litterfall rate constant given by De Vries *et al.* (1994b). Nutrient cycling factors (*ncf*), the fraction of roots in the litterlayer ($fr_{rt\ lt}$) and mineralization constants for forest were taken from a literature survey by De Vries *et al.* (1990), assuming that the was data related to well drained acid soils (pH≈4). Consequently, based on the pH reduction function the data were multiplied by a factor 2 to derive the maximum values (cf Eq. (42)).

Filtering factors for heathlands and grasslands were assumed to be 1.0 because the parameterization of the DEADM model for a 5 x 5 km^2 grid cell is dominated by short vegetation. Dry deposition factors, foliar uptake fractions and foliar exudation fractions for heather and grassland were derived from Bobbink and Heil (1993) and Bobbink *et al.* (1990), respectively. Interception fractions for both vegetation structures were derived from De Visser and De Vries (1989).

As with forests, the amounts of litterfall in heathlands and grasslands were calculated as the product of average values of above ground biomass and litterfall rate constants, using data from Berendse (1988) for *Erica* (wet heathland) and *Molinia* (grass). Reallocation factors, nutrient cycling factors, nutrient contents in above ground biomass and mineralization constants were derived from the same source. The fraction of roots in the humus layer in heathlands was based on Tinhout and Werger (1988). Actually, these authors found that about 75% of the fine root biomass (cf Table 13)

was concentrated in the top 5 cm of the soil. In this model application we assumed this amount to occur in the litter layer. The same assumption was made for grassland. Concentrations of monovalent base cations (K^+) in above-ground biomass in heathlands and grasslands were based on Heil and Diemont (1983) and Bobbink *et al.* (1990), respectively. Values for divalent base cations (Ca^{2+}, Mg^{2+}) were derived from Pruyt (1984). Mineralization constants for heather and grassland were based on Berendse (1988) assuming that they relate to well drained soils (no reduction for groundwater level).

Table 13 Values used for the canopy interactions, nutrient cycling, growth uptake and mineralization parameters for the five vegetation types

Parameter	Unit	PIN	SPR	DEC	HEA	GRP
age_{vg}	(yr)	40.0	40.0	40.0	10.0	10.0
age_{lt}	(yr)	80.0	80.0	80.0	10.0	10.0
Canopy Interaction						
$ffSO_2$	(-)	1.40	1.60	1.15	1.00	1.00
$ffNH_3$	(-)	1.30	1.50	1.10	1.00	1.00
$ffNO_x$	(-)	0.85	1.00	0.70	1.00	1.00
f_{dd}	(-)	2.50	3.00	2.00	1.50	1.50
fr_{int}	(-)	0.30	0.40	0.20	0.10	0.05
$frNH_{4\,fu}$	(-)	0.30	0.30	0.30	0.40	0.30
frH_{fu}	(-)	0.30	0.30	0.30	0.40	0.30
frK_{fe}	(-)	0.63	0.63	0.66	0.65	0.50
Nutrient Cycling						
am_{lf}	(kg m^{-2} a^{-1})	0.41	0.30	0.33	0.24	0.30
ncf	(-)	0.5	0.5	0.5	3.0	3.0
ru_{exp}	(-)	2.0	2.0	2.0	2.0	2.0
fr_{re}	(-)	0.36	0.36	0.36	0.10	0.50
$fr_{rt\,lt}$	(-)	0.25	0.25	0.25	0.75	0.75
$ctBC2_{lv}$	(%)	0.31	0.54	0.64	0.75	0.75
ctK_{lv}	(%)	0.60	0.61	0.92	0.25	0.70
$ctN_{lv\,mn}$	(%)	1.5	1.5	2.5	0.9	1.6
$ctN_{lv\,mx}$	(%)	2.5	2.5	3.5	0.9	1.6
Growth Uptake						
ctN_{st}	(%)	0.12	0.11	0.17	0	0
$ctBC2_{st}$	(%)	0.11	0.08	0.06	0	0
ctK_{st}	(%)	0.05	0.04	0.12	0	0
Mineralization						
$fr_{mi\,mx}$	(-)	0.8	0.8	0.8	0.4	0.8
$k_{mi\,mx}$	(a^{-1})	0.05	0.05	0.05	0.3	0.3

3.5 Data related to soil types

Data used for the soil parameters of the seven soil types are presented in Table 14. To acquire actual transpiration values a soil type dependent transpiration correction factor was introduced, *frpp*. This was done because transpiration values (*tr*) used for the soil vegetation combinations (see Table 15) were derived with a nation wide averaged annual precipitation of 780 mm. In order to account for geographical variability, actual transpiration rates were calculated as (cf Hootsmans and Van Uffelen (1991, internal report):

$$tr_{ac} = tr + frpp \cdot (P - 780) \tag{68}$$

Data on bulk density, soil moisture content, carbonates, CEC, base saturation, organic matter content, total nitrogen content and secondary Al compounds were derived from an extensive field survey of 150 non-calcareous sandy soils (SP and SR; De Vries and Leeters, 1994), about 50 calcareous sandy soils (SC-DLO, W. de Vries, pers. comm), 30 clay soils (CN, CC), 40 loess soils (LN) and 30 peat soils (PN; Klap *et al.*, 1995). Note that all sampling sites were forest site. Exchange constants and the Al equilibrium constant were calculated with Eq. (7), (8) and (13)., using the measured adsorbed and dissolved concentrations of H^+, Al^{3+} and BC^{2+} averaged of the considered soil depth. Here we present the median values related to the root zone for forest, which was set equal for all forest types. Similarly KAl_{ox} derived from averaged soil solution concentrations of Al^{3+} and H^+ for sites with a pH below 4.5. The pH criterion was also used for the calculation of the exchange constant and was introduced to prevent from unrealistic values. Values for the short vegetation may differ considerably in some cases, because the root zone of this vegetation type is only 20 cm, whereas the root zone of the considered forests is always more than 50 cm.

Values for the maximum denitrification fraction ($fr_{de\,mx}$) and the parameters relating denitrification to water-table ($rf_{de\,MSW\,mn}$ and a_{de}) were derived from Breeuwsma *et al.* (1991). Values for the nitrification fraction were calculated as a function of the water-table class, using data on deposition and leachate concentrations of NH_4^+ and NO_3^- in the mentioned 300 forest stands on sandy, clay, loess and peat soils, assuming that the NH_4^+ to NO_3^- ratio at the bottom of the root zone can be described as:

$$\frac{cNH_4}{cNO_3} = \frac{(1 - fr_{ni}) \cdot NH_{4\,td}}{NO_{3\,td} + (1 + fr_{ni}) \cdot NH_{4\,td}} \tag{69}$$

or:

$$fr_{ni} = \frac{\dfrac{NH_{4\,td}}{NO_{3\,td}} - \dfrac{cNH_4}{cNO_3}}{\dfrac{NH_{4\,td}}{NO_{3\,td}} \cdot \left(1 + \dfrac{cNH_4}{cNO_3}\right)} \tag{70}$$

When deposition data for NH_4^+ and NO_3^- were not available, a ratio of 2 was assumed between $NH_{4\,td}$ and $NO_{3\,td}$. The results for the various sandy soils were lumped, because differences appeared to be small. Using these data, a linear relationship between the nitrification fraction and *MSW* was assumed, cf Eq. (61), and values for $fr_{ni\,mx}$, $rf_{ni\,MSW\,mn}$, a_{ni}, b_{ni}, $z1$ and $z2$ were derived as given in Table 14.

The SO_4^{2-} sorption capacity was set equal to 2% of the secondary Al compounds content (Johnson and Todd, 1983). The partial CO_2 pressure was derived from Koorevaar *et al.* (1983). Weathering rates of base cations for the non-calcareous sandy soils were taken from De Vries (1994), who derived weathering rates on the

basis of one-year batch experiments that were scaled to field observations. Weathering rates for calcareous soils were derived from De Vries *et al.* (1994c). For peat and loess soils weathering rates were derived from Van Breemen *et al.* (1984) and Weterings (1989, internal report) respectively. Note, however, that these weathering rates refer to silicate weathering. The weathering in calcareous soils is of course fully dominated by carbonate weathering, cf Eq. (12).

Table 14 Values used for the soil parameters for the seven soil types, related to the depth of the root zone for forest

Parameter	Unit	SP	SR	SC	CN	CC	LN	PN
Depth	(m)	0.70	0.60	0.80	1.00	1.00	1.00	0.50
frpp	(-)	0.10	0.20	0.20	0.0	0.0	0.20	0
ρ_{rz}	(g cm^{-3})	1.45	1.26	1.62	1.16	1.16	1.52	0.17
ρ_{lt}	(g cm^{-3})	0.13	0.13	0.13	0.13	0.13	0.13	0.13
θ	(m^3 m^{-3})	0.13	0.18	0.061	0.27	0.27	0.41	0.84
$ctCa_{cb}$	(mmol$_c$ kg^{-1})	0.	0.0	182.4	0.0	109.0	0.0	0.0
CEC	(mmol$_c$ kg^{-1})	11.3	41.4	7.89	318.9	318.9	53.7	414.1
om	(kg kg^{-1})	0.016	0.061	0.005	0.072	0.070	0.029	0.901
CN_{mn}	(kg kg^{-1})	10.	10.	10.	10.	10.	10.	10.
CN_{cr}	(kg kg^{-1})	30.	30.	20.	30.	20.	30.	30.
CN_{om}	(kg kg^{-1})	21.	26.	10.	10.	10.	21.	35.
DA_{mo}	(kg kg^{-1})	1.5	1.5	1.5	1.5	1.5	1.5	1.5
KAl_{ex}	(log(mol l^{-1}))	0.79	0.16	-1.23	-3.38	-3.38	0.60	-2.14
KH_{ex}	(log(mol l^{-1}))	4.0	3.8	5.04	6.73	6.73	4.23	3.49
KAl_{ox}	(log(mol l^{-1}))	8.1	7.9	8.1	9.4	9.4	8.3	6.45
$frBC2_{ac}$	(-)	0.07	0.06	0.83	0.89	0.89	0.16	0.58
$fr_{ni\ mx}$	(-)	1.0	1.0	1.0	1.0	1.0	1.0	1.0
$rf_{ni\ MSW\ mn}$	(-)	0.3	0.3	0.3	0.5	0.5	0.5	0.3
a_{ni}	(-)	-0.2	-0.2	-0.2	0.5	0.5	0.35	-0.7
b_{ni}	(m^{-1})	2.0	2.0	2.0	1.0	1.0	0.7	1.4
z1	(m)	0.10	0.10	0.10	0.00	0.00	0.20	0.50
z2	(m)	0.50	0.50	0.50	0.50	0.50	0.85	0.85
$fr_{de\ mx}$	(-)	0.90	0.90	0.90	1.0	1.0	0.90	1.0
$rf_{de\ MSW\ mn}$	(-)	0.25	0.25	0.25	0.70	0.70	0.70	0.85
a_{de}	(m^{-1})	0.5	0.5	0.5	0.5	0.2	0.2	0.1
$ctAl_{ox}$	(mmol$_c$ kg^{-1})	84.9	108.5	8.8	196.3	196.3	154.6	101.1
SSC	(mmol$_c$ kg^{-1})	1.7	2.2	0.18	3.9	3.9	3.1	3.1
$C_{1/2}$	(mol$_c$ m^{-3})	1.0	1.0	1.0	1.0	1.0	1.0	1.0
*p*CO2	(hPa)	0.033	0.033	0.033	0.067	0.067	0.033	0.0167
$BC2_{we}$	(mol$_c$ m^{-3} a^{-1})	0.011	0.020	0.010	0.040	0.040	0.020	0.020
K_{we}	(mol$_c$ m^{-3} a^{-1})	0.009	0.025	0.008	0.030	0.030	0.015	0.010
Na_{we}	(mol$_c$ m^{-3} a^{-1})	0.009	0.025	0.008	0.030	0.030	0.015	0.010

3.6 Data related to soil-vegetation combinations

Model parameters that depend on both soil type and vegetation type refer to the depth of the root zone, transpiration rate and growth parameters. Values used for each combination of soil type and vegetation type are given in Table 15.

Table 15 Values used for the soil and vegetation-dependent parameters for all soil vegetation combinations

Soil Vegetation Combination	T_{rz} (m)	Tr (m a^{-1})	k_{gl} (a^{-1})	$t_{½}$ (yr)	$Am_{st\ mx}$ (kg m^{-2})
SPPIN	0.7	0.276	0.067	40.0	22.24
SRPIN	0.6	0.292	0.066	39.0	28.31
SCPIN	0.8	0.298	0.085	34.0	10.51
CNPIN	1.0	0.378	0.085	34.0	10.51
CCPIN	1.0	0.378	0.085	34.0	10.51
LNPIN	1.0	0.282	0.066	39.0	28.31
PNPIN	0.5	0.378	0.085	34.0	10.51
SPSPR	0.7	0.296	0.072	38.0	25.02
SRSPR	0.6	0.304	0.077	37.0	41.08
SCSPR	0.8	0.329	0.072	38.0	25.02
CCSPR	1.0	0.417	0.072	38.0	25.02
PNSPR	0.5	0.417	0.072	38.0	25.02
LNSPR	1.0	0.306	0.077	37.0	41.08
SPDEC	0.7	0.326	0.088	50.0	28.77
SRDEC	0.6	0.328	0.088	48.0	76.93
SCDEC	0.8	0.34	0.088	48.0	76.93
CNDEC	1.0	0.397	0.090	49.0	49.91
CCDEC	1.0	0.397	0.088	48.0	76.93
LNDEC	1.0	0.326	0.088	48.0	76.93
PNDEC	0.5	0.397	0.090	49.0	49.91
SPHEA	0.2	0.335	0.15	10	1.4
SRHEA	0.2	0.37	0.15	10	1.4
SCHEA	0.2	0.335	0.15	10	1.4
CNHEA	N/A[1)]				
CCHEA	N/A[1)]				
LNHEA	N/A[1)]				
PNHEA	0.2	0.41	0.15	10	1.4
SPGRP	0.2	0.40	0.15	5	0.5
SRGRP	0.2	0.44	0.15	5	0.5
SCGRP	0.2	0.40	0.15	5	0.5
CNGRP	0.2	0.48	0.15	5	0.5
CCGRP	0.2	0.48	0.15	5	0.5
LNGRP	0.2	0.44	0.15	5	0.5
PNGRP	0.2	0.48	0.15	5	0.5

[1)] Soil-vegetation combination that do not occurs

The thickness of the root zone and actual evapotranspiration rates for forest were taken from De Vries *et al.* (1994c), who derived transpiration fluxes from model calculations (SWATRE, Belmans *et al.*, 1983) for various forest types on sandy soils, while using expert judgement for forests on peat, loess and clay soils. Actual evapotranspiration rates for short vegetation on sandy soils were derived from De Visser and De Vries (1989). Values for loess soils were assumed to equal those for rich sandy soils. Values for clay and peat soils were set equal to potential evapotranspiration rates as given in De Visser and De Vries (1989). Growth rate parameters for forest were based on a literature survey presented by De Vries *et al.* (1990). Growth rates for short vegetation refer to shoot growth only (i.e. increase in litterfall), and were derived from Berendse (1988). The increase of non shoot material (i.e. stems in the model) was assumed to be negligible. This was mimicked in the model by setting the nutrient contents in stems to zero (cf. Table 13).

4 Results and discussion

In this Chapter the results are presented from an indicative application of the model SMART2 on a national scale. Presented results are mainly restricted to the model outputs necessary for MOVE applications, i.e. pH and N availability. Here, the N availability is defined as the sum of the N throughfall flux and the N mineralization flux (cf 2.3.1). Although the base saturation as such is not an input for the MOVE model, it is also presented because of its (hydro)ecological implication. In order to validate the model some other outputs are presented as well.

Note that there was no hydrological input (i.e. mainly the seepage flux; output from the LGM model) available for the western part of the Netherlands (cf Section 3.3.2.1 and Annex 2). However, it was decided to present model results for the Netherlands as a whole. Therefore for those grids for which no seepage data were available a seepage flux of nil was assumed.

4.1 Geographical distribution of pH and nitrogen availability

The geographic distribution of the dominant pH and nitrogen availability per grid cell for each vegetation type in the year 1990 and 2050 for Deposition Scenario 2 (i.e. reducing deposition) and Seepage Scenario 2 (increasing seepage) are presented in Figures 4 to 8.

Results showed a highly spatial variability in pH, which was mainly determined by the location of soil types. Calcareous sandy soils and clay soils along the coast-line, clay soils in along the rivers are well buffered soils, resulting in relatively high pH values. Non-calcareous sandy soils in the central part and the southern part of the country have a lower buffer capacity, resulting in relatively low pH values. Figures 4 to 8 show that deposition reductions and seepage increase result in an increase in pH values, especially for the non-calcareous soils.

For forest results also showed a significant decrease in N availability in 2050 compared to 1990. Results on N availability also showed a highly spatial variability, which was, in contrary to the pH, due to the spatial variability in atmospheric N deposition. N availabilities appeared to be high in the central part and the southern part of the country, which are areas with high atmospheric deposition of N, whereas in the northern part of the country the atmospheric deposition of N is low which resulted in lower N availabilities. Contrary to forest, the N availability for heather and grassland showed an increase in N availability during the simulation period. This increase was due to a serious increase in N mineralization fluxes which exceeded the reductions in N deposition (cf. section 4.2). The increase in mineralization fluxes was mainly caused by the increase in litterfall. For heather and grassland it was assumed that they were only 10 years old in 1990 (cf. section 3.4), which means that the litterfall will double for heather and increase with 50% for grassland during the next 50 years.

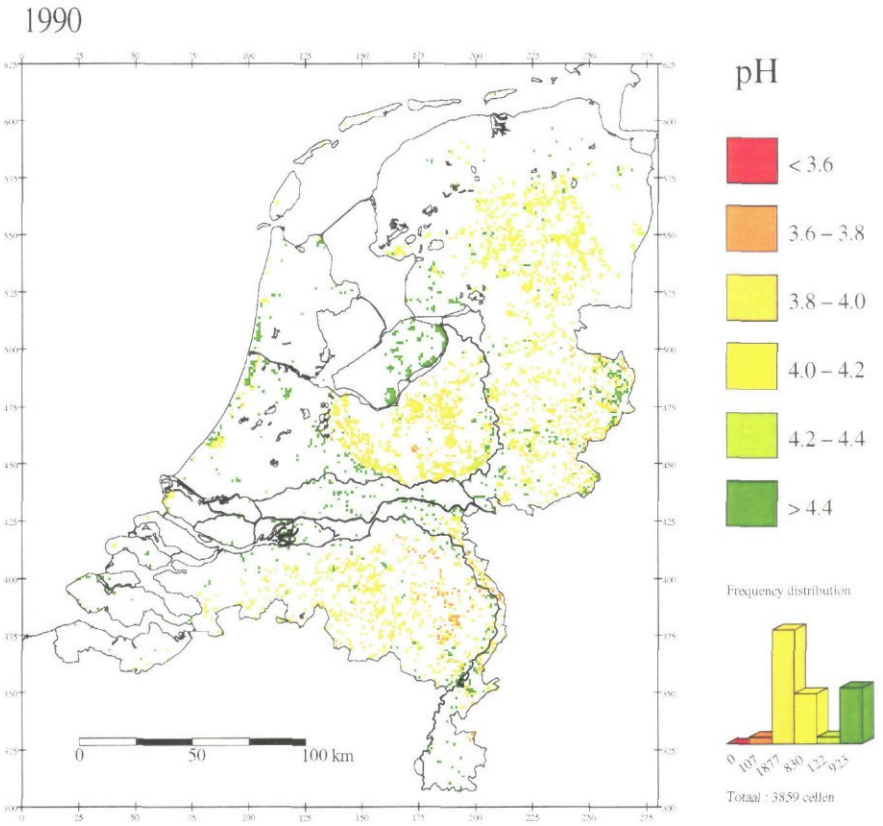
1990
pH
< 3.6
3.6 – 3.8
3.8 – 4.0
4.0 – 4.2
4.2 – 4.4
> 4.4
Frequency distribution
0
107
1877
830
122
923
Totaal : 3859 cellen
0
50
100 km

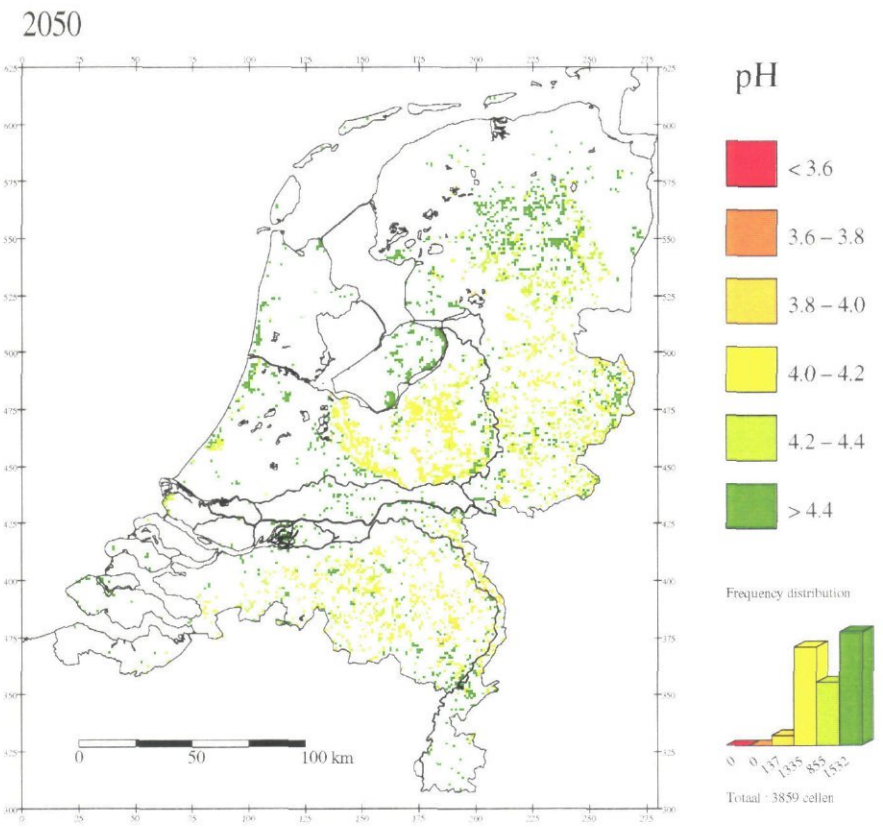
2050
pH
< 3.6
3.6 – 3.8
3.8 – 4.0
4.0 – 4.2
4.2 – 4.4
> 4.4
Frequency distribution
0
0
137
1335
855
1532
Totaal : 3859 cellen
0
50
100 km

Fig. 4a–b

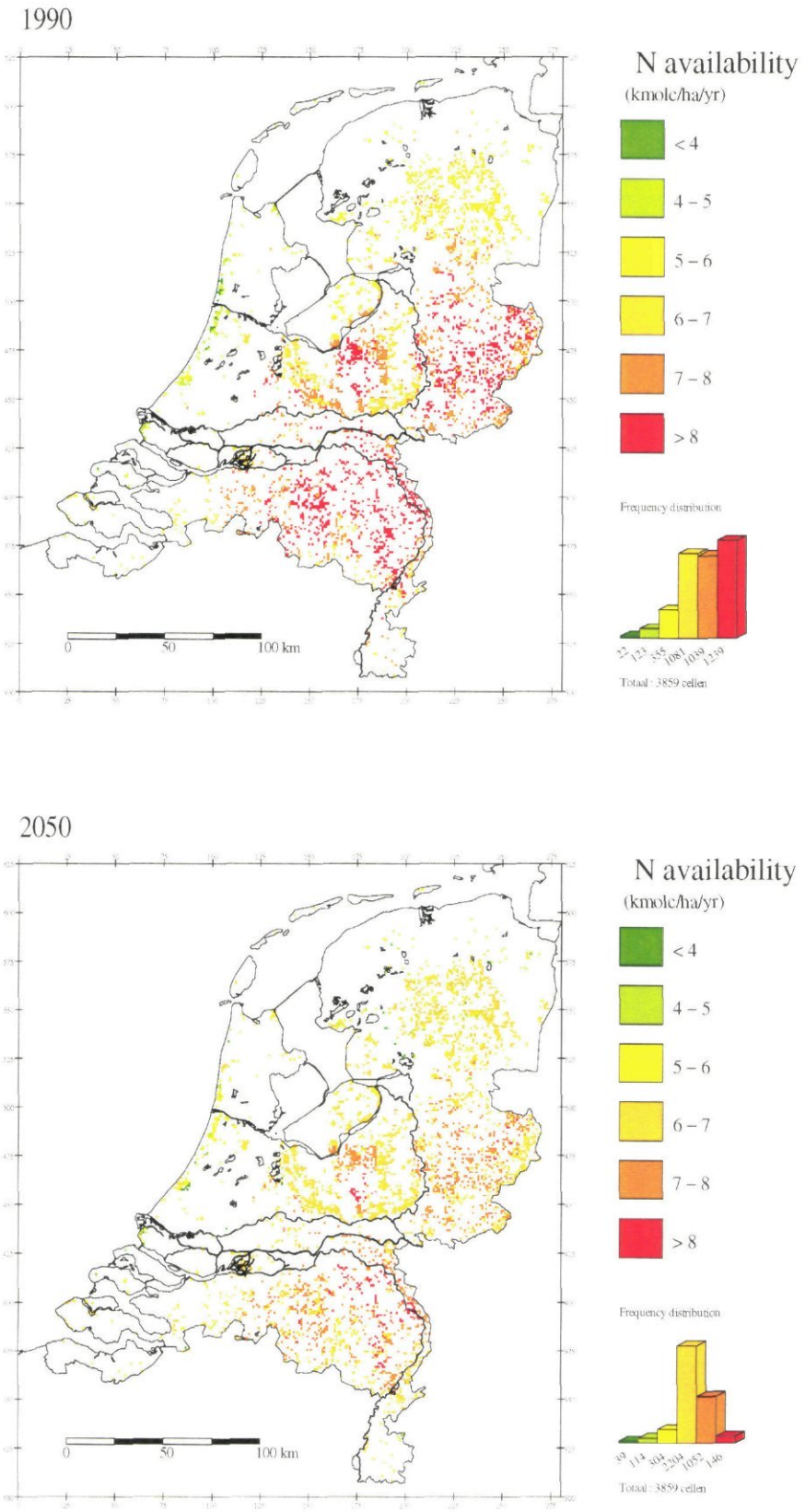

Fig. 4c–d

Fig. 4 Geographical distribution of dominant values for the pH (a, b) and N availability ($kmol_c\ ha^{-1}\ a^{-1}$) (c, d) at the bottom of the root zone of deciduous forest in 1990 (a, c) and 2050 (b, d)

1990

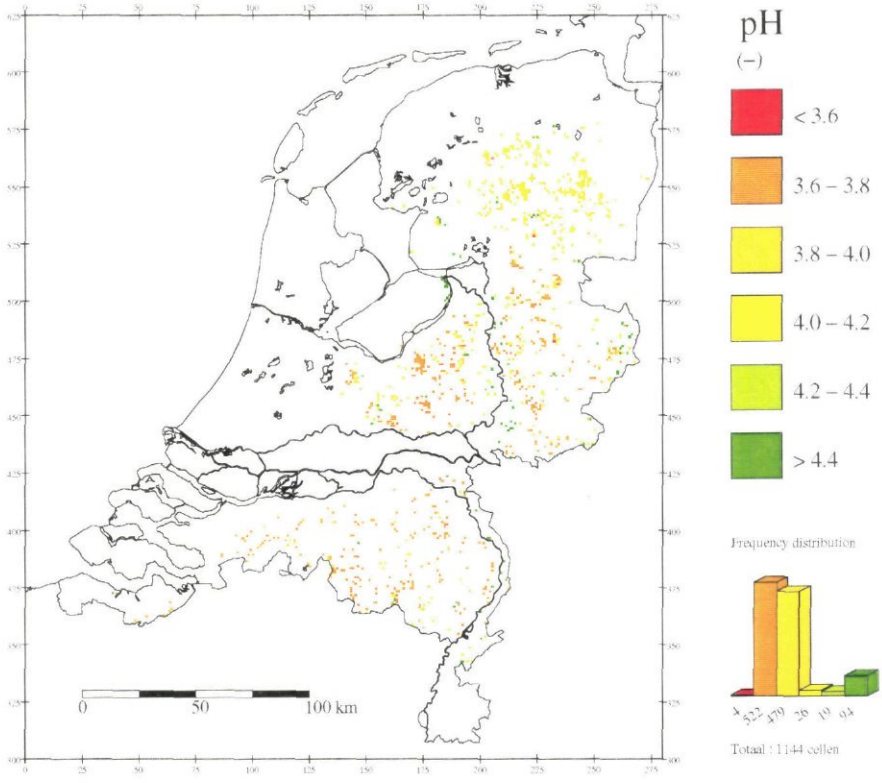

2050

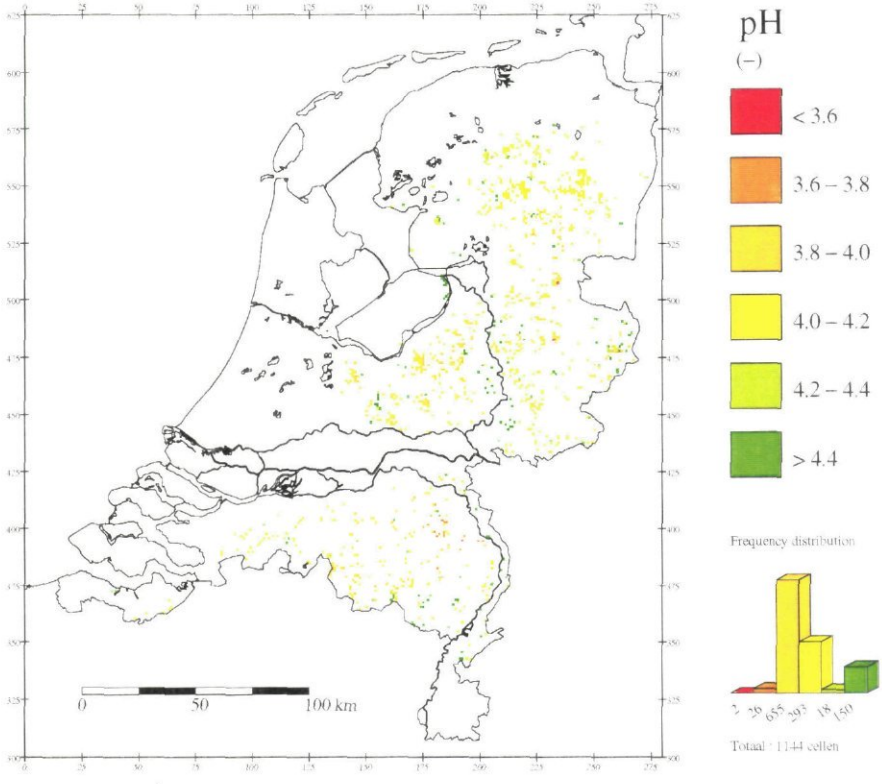

Fig. 5a–b

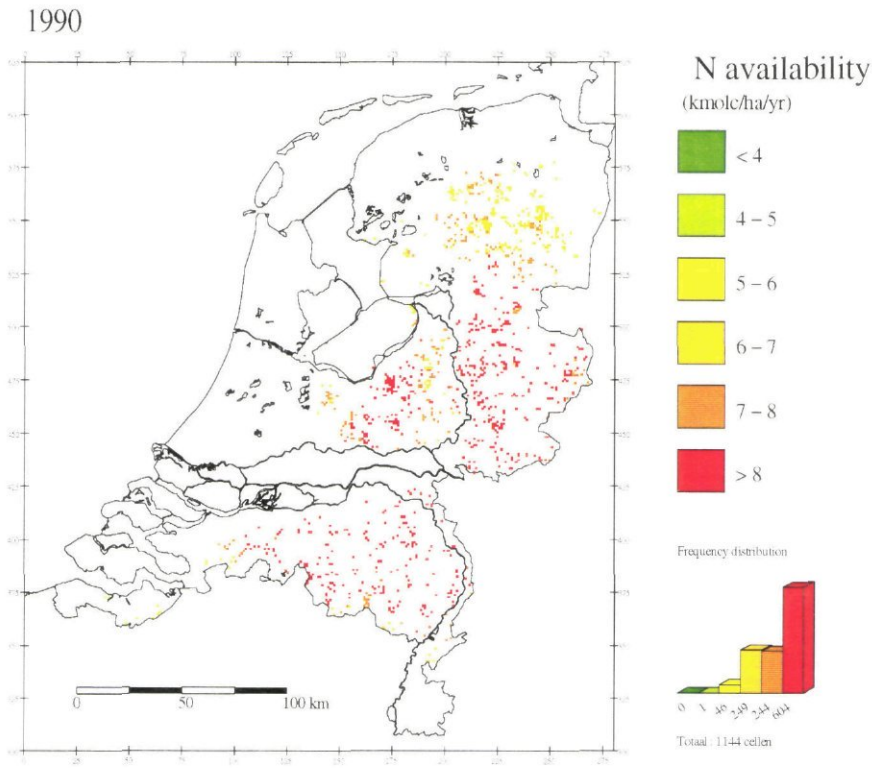

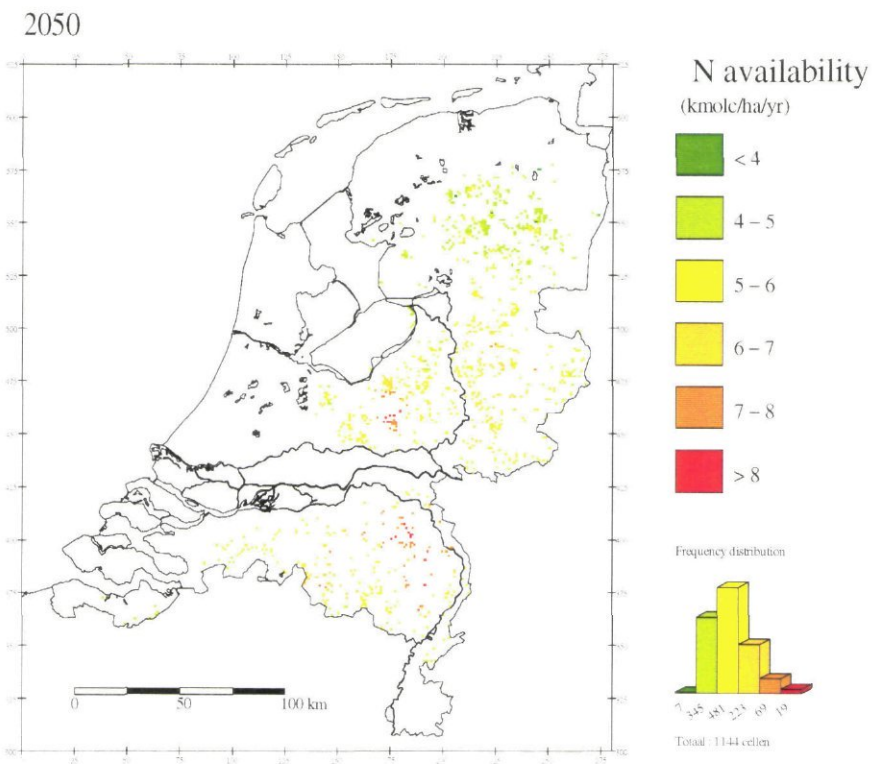

Fig. 5c–d

Fig. 5 Geographical distribution of dominant values for the pH (a, b) and N availability ($kmol_c\ ha^{-1}\ a^{-1}$) (c, d) at the bottom of the root zone of spruce forest in 1990 (a, c) and 2050 (b, d)

1990

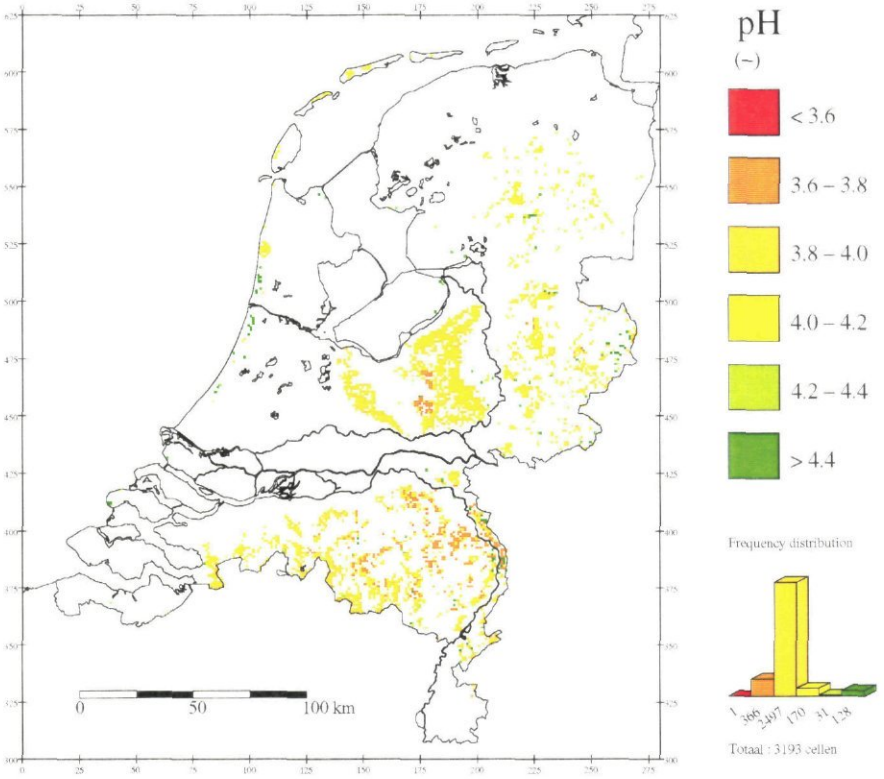

pH
(–)

< 3.6
3.6 – 3.8
3.8 – 4.0
4.0 – 4.2
4.2 – 4.4
> 4.4

Frequency distribution

Totaal : 3193 cellen

2050

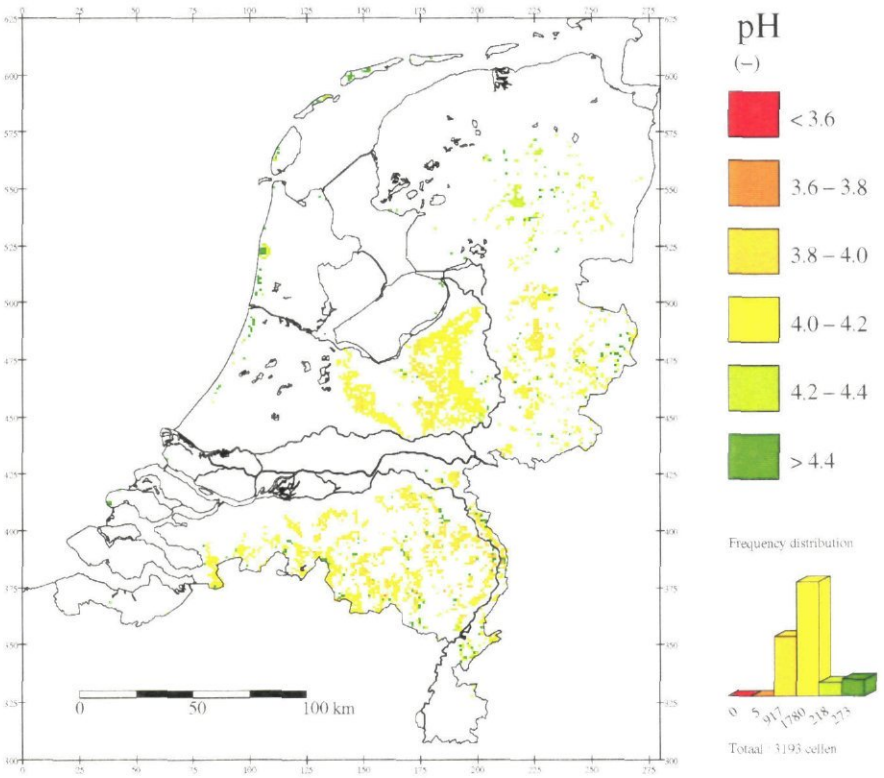

pH
(–)

< 3.6
3.6 – 3.8
3.8 – 4.0
4.0 – 4.2
4.2 – 4.4
> 4.4

Frequency distribution

Totaal : 3193 cellen

Fig. 6a–b

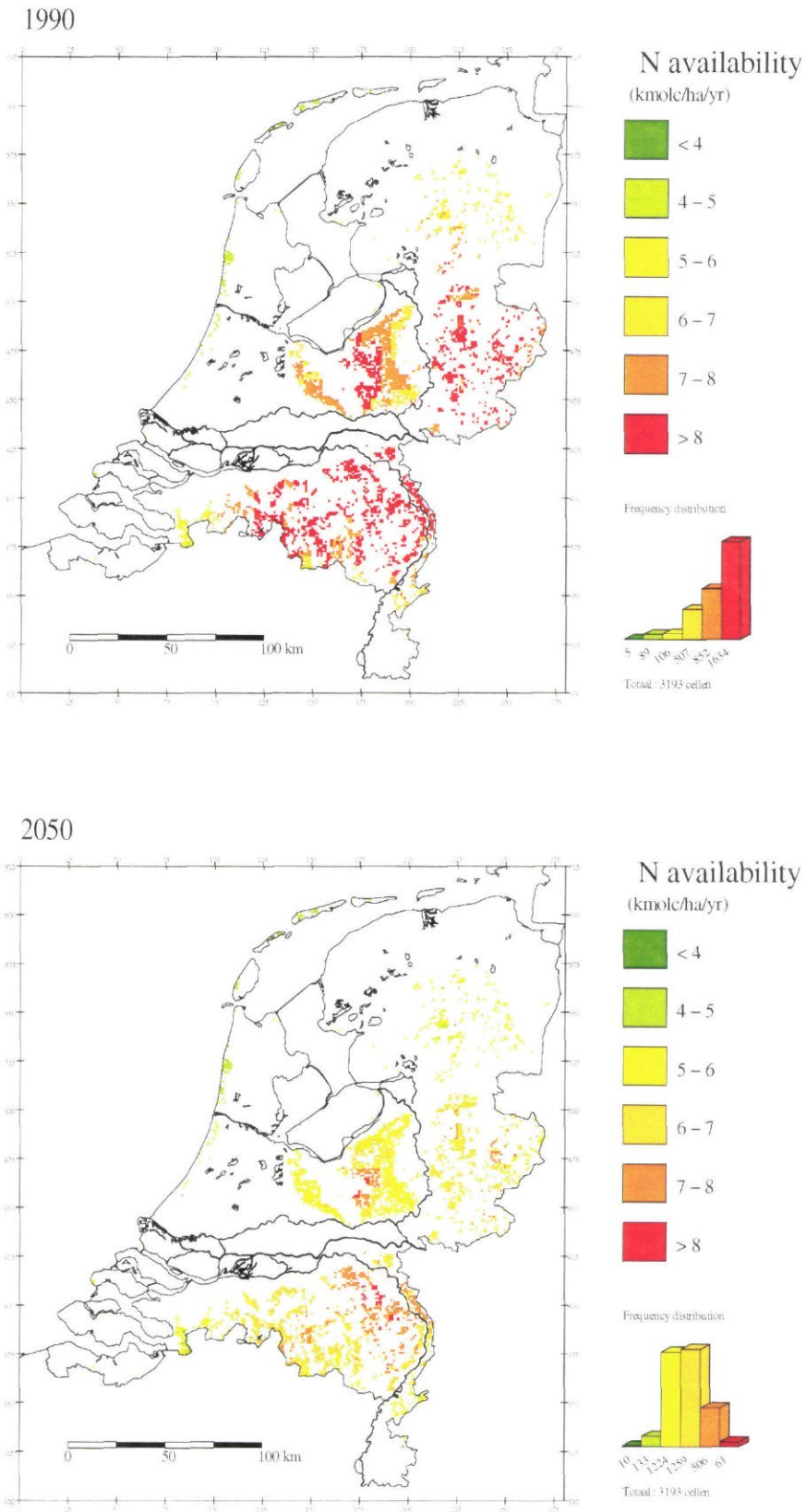

Fig. 6c–d

Fig. 6 Geographical distribution of dominant values for the pH (a, b) and N availability ($kmol_c\ ha^{-1}\ a^{-1}$) (c, d) at the bottom of the root zone of pine forest in 1990 (a, c) and 2050 (b, d)

1990

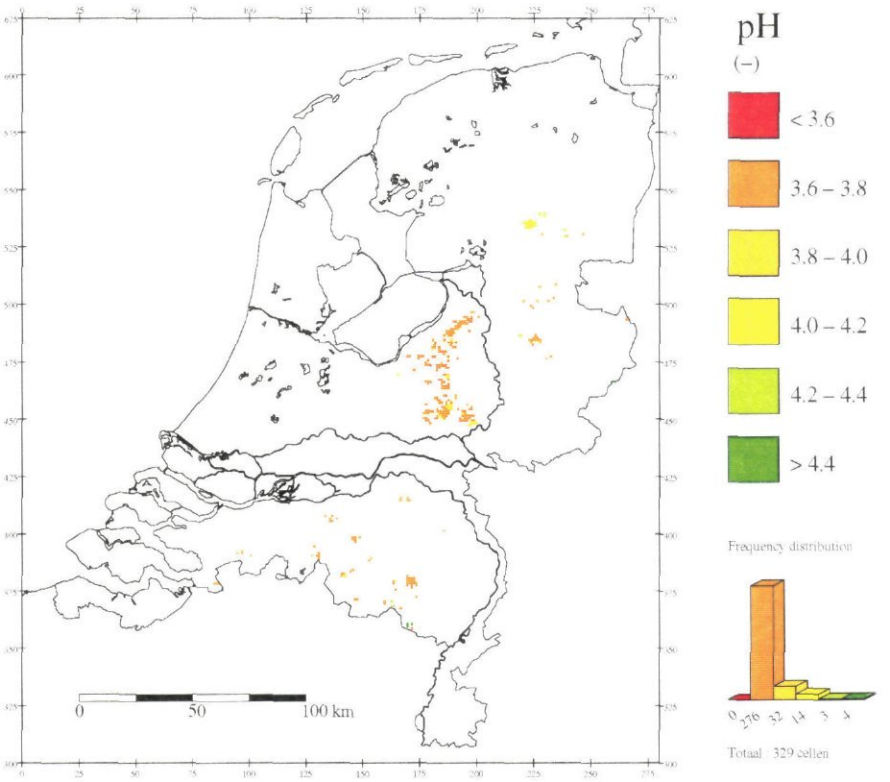

2050

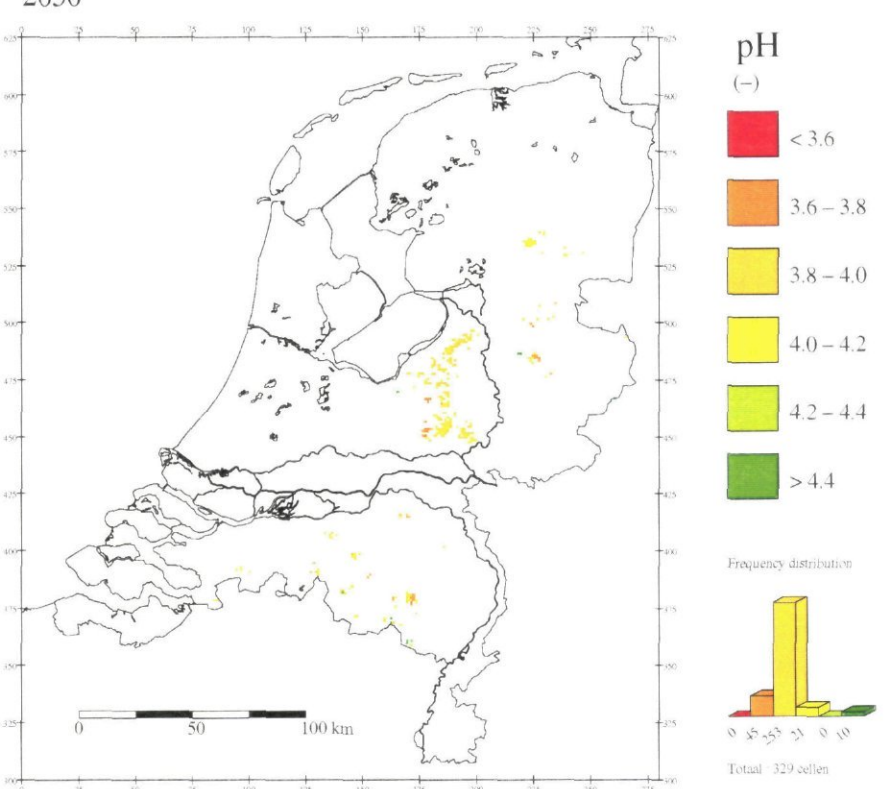

Fig. 7a–b

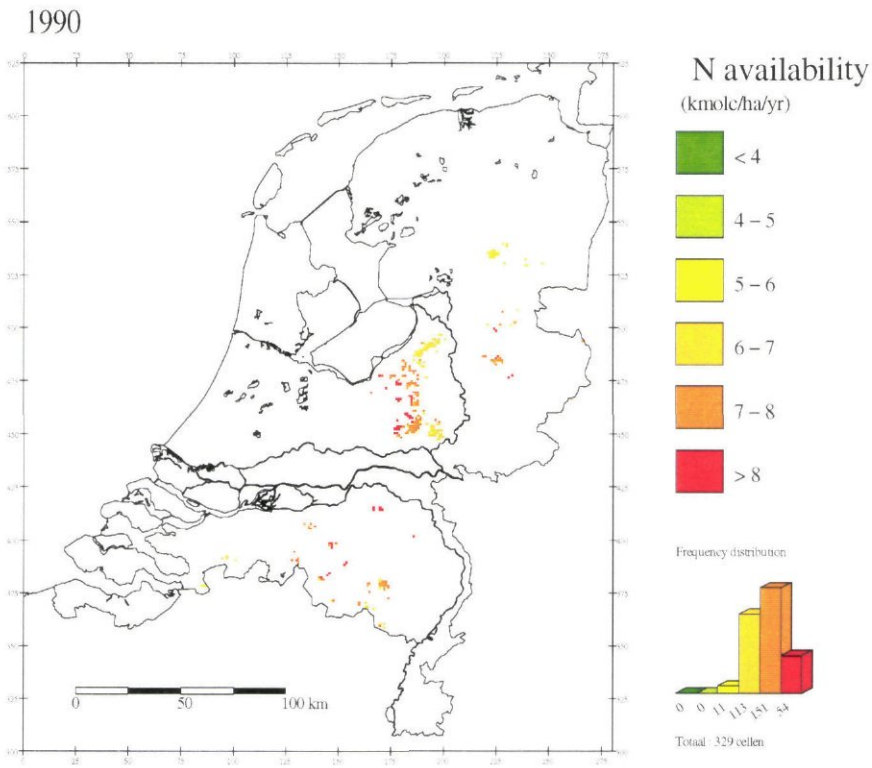

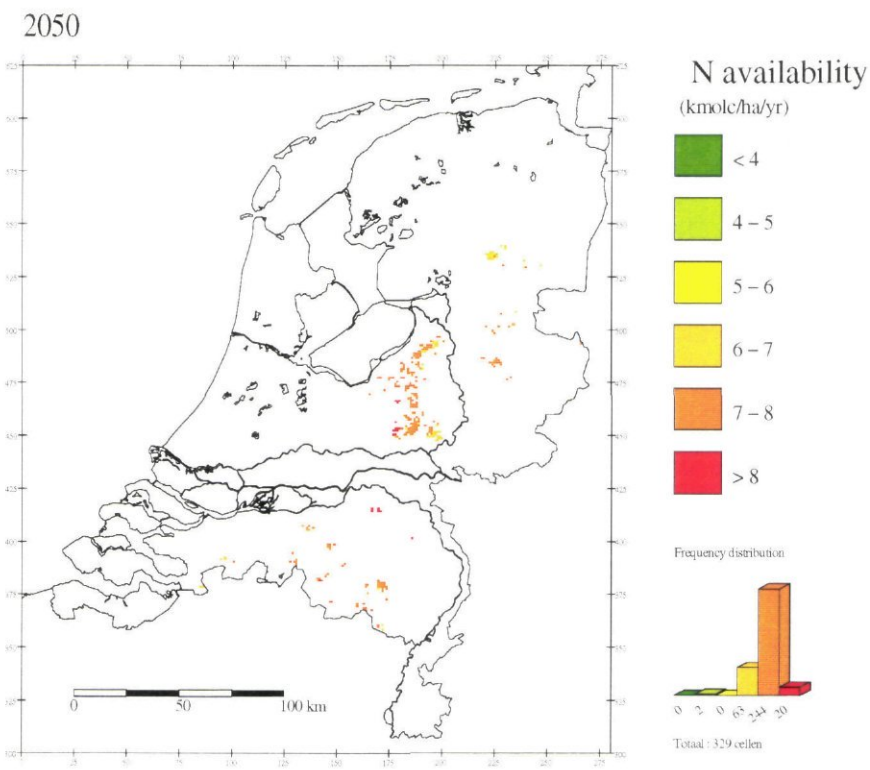

Fig. 7c–d

Fig. 7 Geographical distribution of dominant values for the pH (a, b) and N availability ($kmol_c\ ha^{-1}\ a^{-1}$) (c, d) at the bottom of the root zone of heather in 1990 (a, c) and 2050 (b, d)

1990

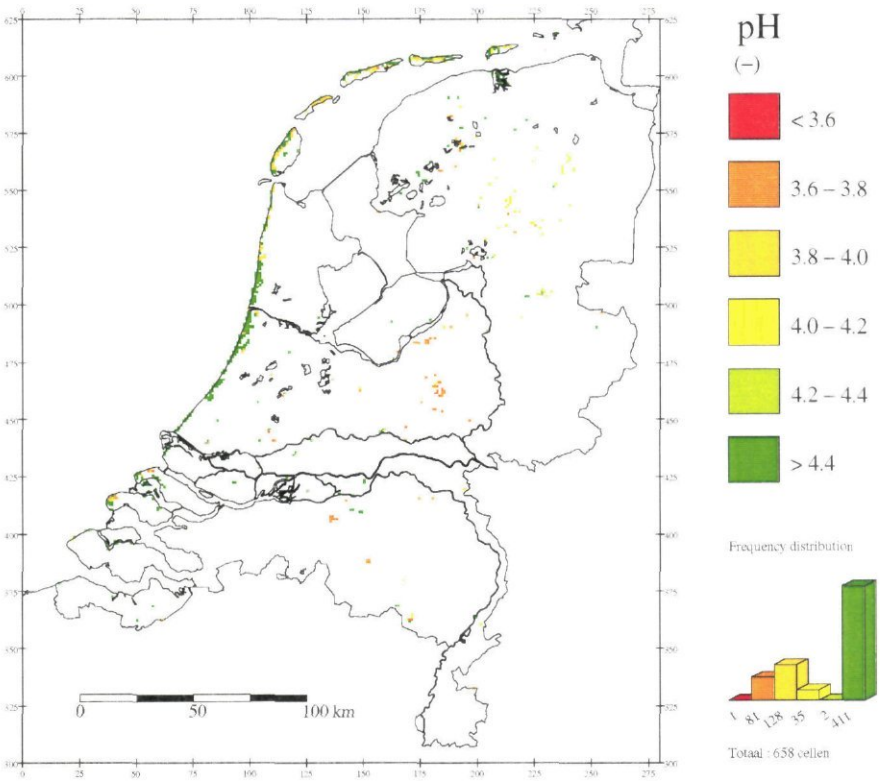

2050

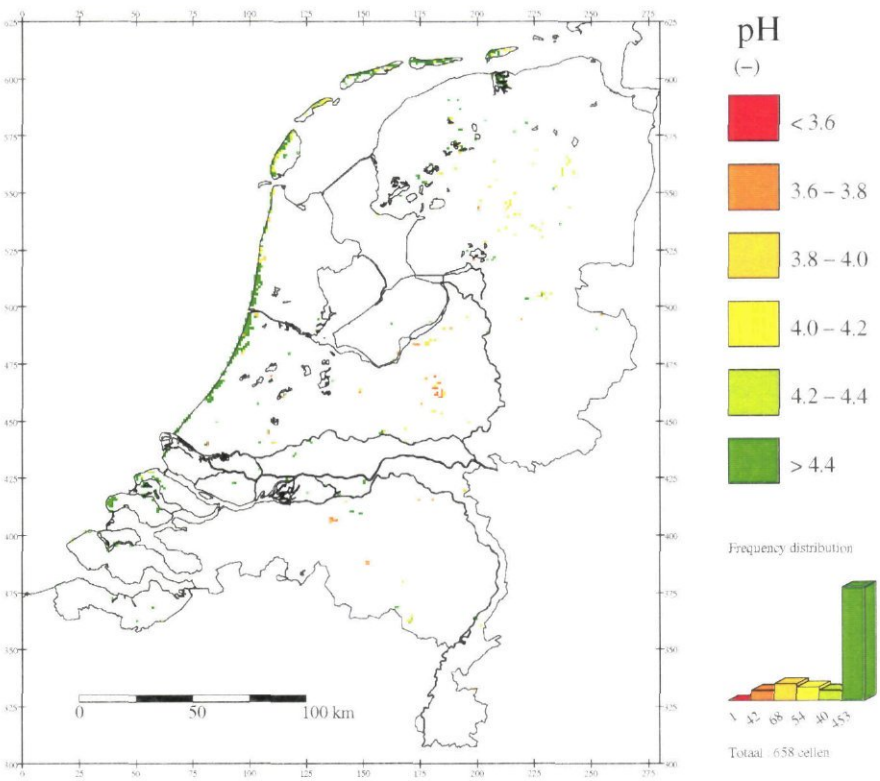

Fig. 8a–b

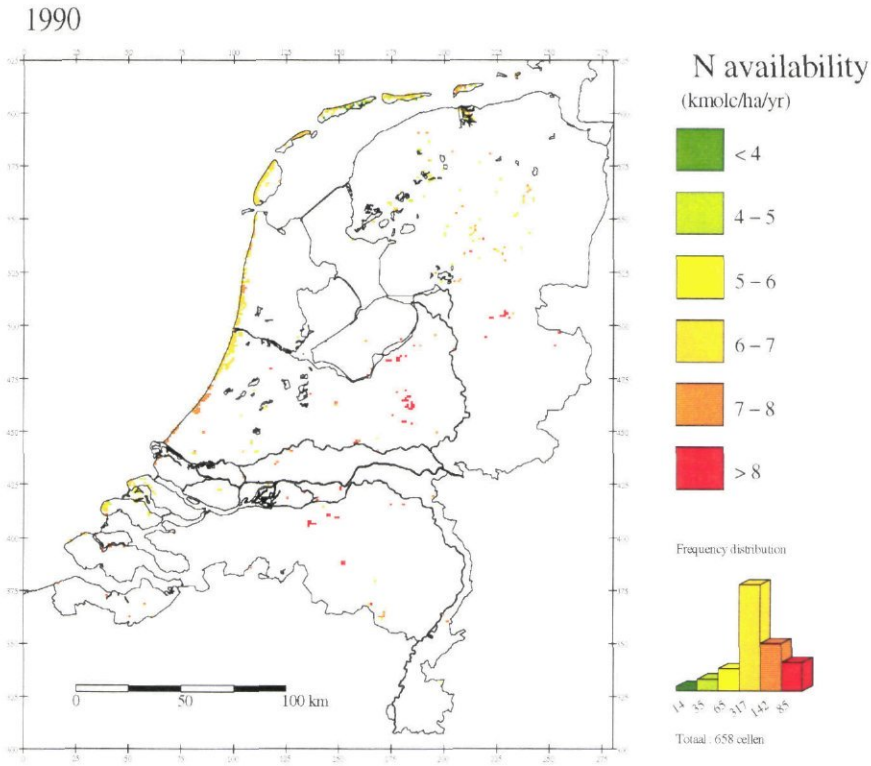

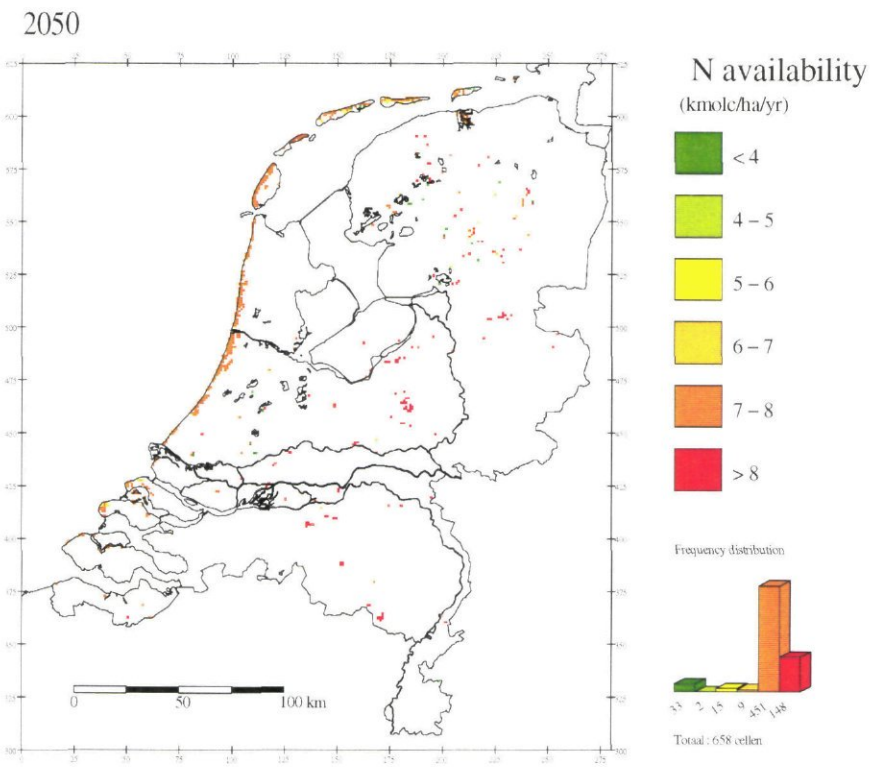

Fig. 8c–d

Fig. 8 Geographical distribution of dominant values for the pH (a, b) and N availability ($kmol_c\ ha^{-1}\ a^{-1}$) (c, d) at the bottom of the root zone of grassland in 1990 (a, c) and 2050 (b, d)

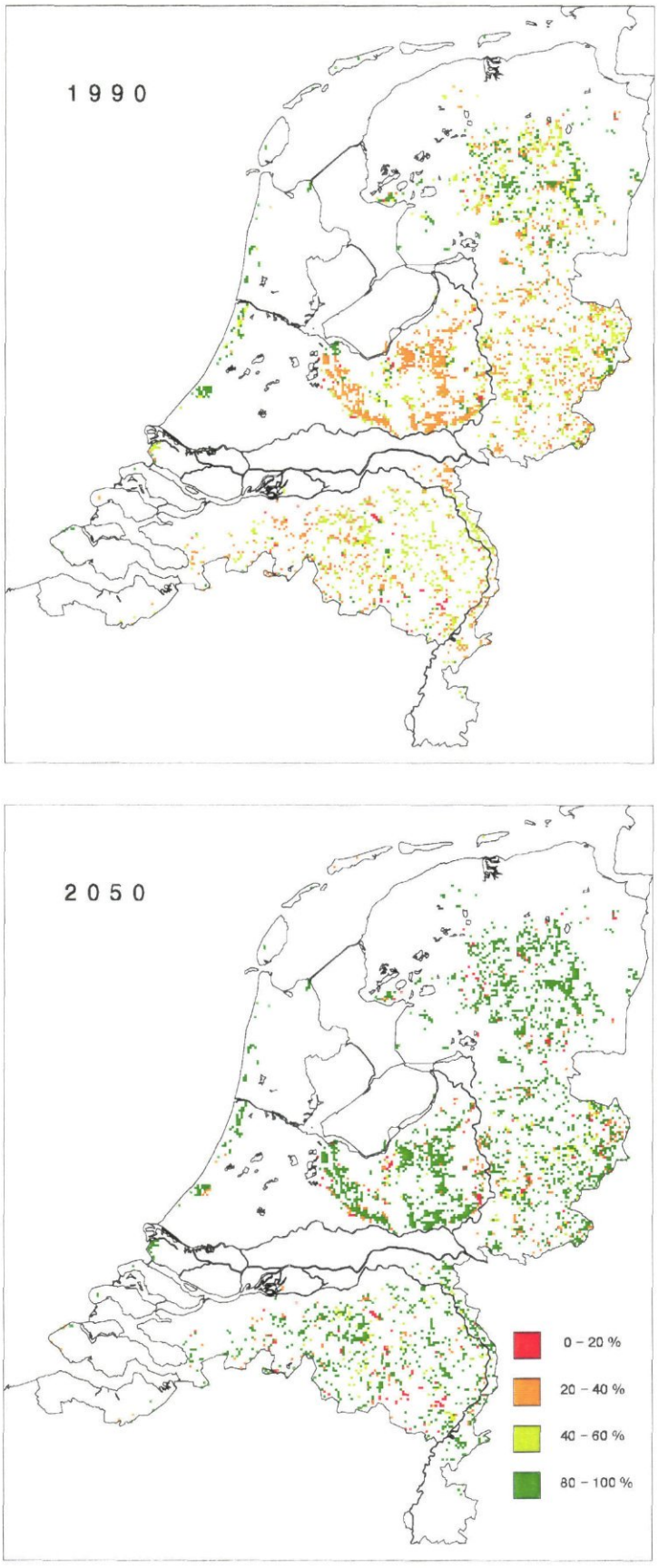

Fig. 9 Predicted geographical distribution of the occurrence probability of plant species in nutrient-poor deciduous forest in 1990 (a) and 2050 (b), in response to Seepage Scenario 2 and Acidification Scenario 2

4.2 Effects of vegetation type, soil type and water-table class on abiotic site factors

The changes in pH and N availability are also illustrated by the Tables 16 and 17. In addition, these tables also present the base saturation. The influence of vegetation type on the site factors is presented in Table 16. Vegetation type influences the soil chemistry by differences in: nutrient cycle, filtering of dry deposition and transpiration. As a result of deposition reduction and seepage increase the pH and base saturation increased, whereas the N availability decreased for forests and increased for short vegetation (heather and grassland). The pH and base saturation increase was rather limited, except for grassland. Grassland also showed higher values for pH and base saturation throughout the simulation period. However, the relatively high pH and base saturation for grassland were biased by the fact that about 45% of the considered sites are located on calcareous sandy soils or clay soils. For other vegetation types the differences in pH and base saturation were generally small. Deciduous forest, though, show a slightly higher pH and a slightly higher base saturation, which was mainly an effect of soil type and water-table class. Compared to coniferous forest, deciduous forest are generally located on richer soils with a higher water-table (i.e. wetter circumstances). The higher base saturation for spruce forest was most likely due to a higher filtering of dry deposition, resulting to an higher input of base cations. For the three forest types the N availability in 2050 was significantly lower than in 1990. In spite of the reduction in N deposition, the N availability in 2010 was lower than in 2050. This was caused by the counteracting effect of a decrease in N deposition and an increase in mineralization. During the period 1990-2010 there was still a significant accumulation of litter in the litterlayer, whereas in 2050 there was more or less a steady-state between litterfall and mineralization. In addition, the litterfall flux also slightly increases during the simulation period, because in 1990 the maximum amount of litterfall was not yet achieved (cf. section 3.4). For spruce forest the mineralization flux increased from 2.9 to 3.1 $kmol_c\ ha^{-1}\ a^{-1}$ during the period 1990-2050, for pine forest from 3.1 to 4.0 $kmol_c\ ha^{-1}\ a^{-1}$ and for deciduous forest from 3.4 to 5.1 $kmol_c\ ha^{-1}\ a^{-1}$. For heather and grassland, the N availability in 2050 was even higher than in 1990, which was due to a serious increase in N mineralization: 3.4 to 5.5 $kmol_c\ ha^{-1}\ a^{-1}$ for heather and 4.4 to 6.8 $kmol_c\ ha^{-1}\ a^{-1}$ for grassland during the period 1990-2050. This huge increase, which exceeded the reduction in N deposition, was mainly caused by an increase in litterfall (cf. section 4.1).

Table 16 Effects of vegetation type on the predicted median pH, N availability and base saturation (BS) in the root zone for all soil types in 1990, 2010 and 2050 in response to Seepage Scenario 2 and Acidification Scenario 2

Vegetation type	$N^{1)}$	pH			N availability ($kmol_c\ ha^{-1}\ a^{-1}$)			BS (%)		
		1990	2010	2050	1990	2010	2050	1990	2010	2050
Spruce	2123	3.8	3.9	3.9	7.9	5.1	5.3	4	4	6
Pine	5566	3.9	4.0	4.0	7.9	5.5	6.0	2	2	3
Deciduous	6971	4.0	4.2	4.2	7.1	5.9	6.6	5	4	6
Heather	463	3.7	3.9	3.8	7.1	6.6	7.2	2	2	3
Grass	1218	4.1	4.3	4.5	6.6	7.4	7.7	36	32	74

[1] *N* represents the number of evaluated combinations

Soil type (Table 17) influences the site factors by differences in weathering rates and cation exchange capacity. The effect of soil type was much more pronounced than the effect of vegetation type. Naturally, a clear distinct exists between calcareous and non-calcareous soils. Calcareous soils have high pH values and base saturation due to the presence of calcite. The N availability of calcareous soils was relatively low, because they are generally located in areas with relatively low atmospheric input of N. Although, due to the relatively low contribution of the N throughfall flux to the N availability for calcareous soils, the reduction in N deposition was overruled by an increase in N mineralization (see also preceding paragraph). Consequently, for these soils the N availability in 2050 was higher than in 1990. The lowest N availability in 2050, though, was found for peat soils which was due to low mineralization fluxes. The median N mineralization flux for peat soils with deciduous forest in 2050 was 3.1 $kmol_c\ ha^{-1}\ a^{-1}$, whereas the average mineralization flux was 5.1 $kmol_c\ ha^{-1}\ a^{-1}$. The non-calcareous sandy soils have the lowest pH and very low base saturation, indicating that these soil are strongly acidified. Even the increase in pH and base saturation as a results of deposition reductions and seepage increase appeared to be small for the non-calcareous sandy soils. For the poor non-calcareous sandy soils, there was even no increase in base saturation when regarding the whole simulation period. For loess soils and peat soils the base saturation was even decreasing, meaning that soil acidification is still going on. For peat soils the combination of a pH around 3.9 and a base saturation around 50% is remarkable, but is in agreement with field observations (Klap *et al.*, 1995).

Regarding the effect of the combined scenario on the pH, the calcareous soils showed no response. These systems are buffered by calcite, that keep the system at a pH of about 7 irrespective of deposition level and seepage input. The other soil types showed an increase of the pH from about 0.1 to 0.3. For all soil types the median N availability remained above the optimum value of 3 $kmol_c\ ha^{-1}\ a^{-1}$ (Latour *et al.*, 1993). For the pH Latour *et al.* (1993) reported an optimum value of 4.2 for nutrient-poor deciduous forest. Results showed for all soils, except the non-calcareous sandy soils and peat soils, a median pH above 4.2 at the end of the simulation period.

Table 17 Effects of soil type on the predicted median pH, N availability and base saturation (BS) in the root zone below deciduous forest in 1990, 2010 and 2050 in response to Seepage Scenario 2 and Acidification Scenario 2

Soil type	$N^{1)}$	pH			N availability ($kmol_c\ ha^{-1}\ a^{-1}$)			BS (%)		
		1990	2010	2050	1990	2010	2050	1990	2010	2050
Sand poor	3166	3.9	4.1	4.1	7.1	5.6	6.7	3	2	3
Sand rich	2283	4.0	4.2	4.2	7.3	5.8	6.6	5	4	7
Sand calc.	184	7.0	7.1	7.1	4.9	4.2	5.8	100	100	100
Peat	375	3.8	3.9	3.9	6.9	5.0	5.2	51	49	47
Loess	72	4.2	4.5	4.4	7.6	6.1	6.7	14	13	13
Clay	554	5.9	6.0	6.0	8.2	6.4	6.9	89	88	88
Clay calc.	337	6.8	6.8	6.9	6.2	5.3	6.5	100	100	100

[1] *N* represents the number of evaluated combinations

4.3 Effects of deposition and seepage scenarios on abiotic site factors

Regarding the effect of deposition reductions alone (Table 18 and 19; compare the columns 11 vs. 21 and 12 vs. 22), it can be concluded that deposition reductions will lead to an increase in median values of pH and base saturation and a decrease in N availability. Although, the pH increase was rather small, 0.1 - 0.5 pH. The same was true for base saturation. The largest changes occurred in grassland (cf. Table 19), whereas the effects of deposition reduction on pH and base saturation were negligible small for the well buffered calcareous soils. The reduction in N availability was moderate compared to the reduction in N deposition: reductions from 20 to 40%, whereas the average reduction in N deposition was more than 50% (cf. Table 9).

The changes in pH and base saturation were also relatively small compared to another study on the evaluation of a similar deposition scenario (cf. De Vries *et al.*, 1994). The main reason for this, is that this study presents results from the one box model SMART2 representing the root zone as one box, whereas De Vries *et al.* (1994) presented results from the multi layer model RESAM focusing on the top 30 cm, i.e. the layer where the major changes in pH and base saturation occur. Using one large compartment (up to 1 m), as was done in this study, changes in pH and base saturation were averaged out. The results on N availability, though, were not influenced by the thickness of the soil compartment, because this output refers to a flux for the root zone (including the litterlayer) as whole.

Regarding the effects of seepage increase (Table 18 and 19; compare the columns 11 vs. 12 and 21 vs. 22), it can be concluded that there is no effect on the median values of pH, N availability and base saturation. With respect to the effects of Seepage Scenario 2, the results of Table 18 should be handled with care. The surface area that is affected by Seepage Scenario 2 is relatively small, whereas deposition scenario affects all systems. Seepage increase only affects locations in the surroundings of groundwater abstraction wells and is restricted to sites with water-table class 1, 2 and 3 (cf Section 3.3.2.1). When focusing on these sites, however, the effect of Seepage Scenario 2 on the median values is still negligible (Results not shown). Realizing that seepage increase only occurred in 3088 grid cells (i.e.

9% of the surface area of the Netherlands, cf.3.3.2.1) with an average increase of only 50 mm a^{-1}, this result is not surprising.

Table 18 Effects of combinations of the various scenarios[1] on the predicted median pH, N availability and base saturation (BS) in the root zone below deciduous forest, for the different soil types in 2050

Soil type	N[2]	pH				N availability ($kmol_c$ ha^{-1} a^{-1})				BS (%)			
		11	12	21	22	11	12	21	22	11	12	21	22
Sand poor	3166	3.9	3.9	4.1	4.1	9.3	9.3	6.7	6.7	1	1	3	3
Sand rich	2283	3.9	3.9	4.2	4.2	9.3	9.3	6.6	6.6	2	2	7	7
Sand calc.	184	7.0	7.0	7.1	7.1	7.3	7.3	5.8	5.8	100	100	100	100
Peat	375	3.6	3.6	3.9	3.9	8.8	8.8	5.2	5.2	37	37	47	47
Loess	72	4.1	4.1	4.4	4.4	9.4	9.4	6.7	6.7	6	6	13	13
Clay	554	5.8	5.8	6.0	6.0	9.5	9.5	6.9	6.9	87	87	88	88
Clay calc.	337	6.8	6.8	6.9	6.9	8.7	8.7	6.5	6.5	100	100	100	100

1) The first digit refers to the deposition scenario, the second digit refers to the Seepage Scenario, e.g. 21 refers to Deposition Scenario 2 and Seepage Scenario 1

2) *N* represents the number of evaluated combinations

Table 19 Effects of combinations of the various scenarios[1] on the predicted median pH, N availability and base saturation (BS) in the root zone off all soil type for the different vegetation types in the year 2050

Soil type	N[2]	pH				N availability ($kmol_c$ ha^{-1} a^{-1})				BS (%)			
		11	12	21	22	11	12	21	22	11	12	21	22
Spruce	2123	3.7	3.7	3.9	3.9	9.3	9.3	5.3	5.3	2	2	3	3
Pine	5566	3.8	3.8	4.0	4.0	9.6	9.6	6.0	6.0	1	1	3	3
Deciduous	6971	3.9	3.9	4.2	4.2	9.2	9.2	6.6	6.6	2	2	6	6
Heather	463	3.7	3.7	3.8	3.8	9.2	9.2	7.2	7.2	1	1	3	3
Grass	1218	4.0	4.0	4.5	4.5	8.6	8.6	7.7	7.7	23	23	74	74

1) The first digit refers to the deposition scenario, the second digit refers to the Seepage Scenario, e.g. 21 refers to Deposition Scenario 2 and Seepage Scenario 1

2) *N* represents the number of evaluated combinations

4.4 Model validation

4.4.1 Soil solution concentrations

In order to gain insight into the reliability of the model predictions, model results of the soil and solution chemistry for forest were compared to soil and soil solution measurements at 60-100 cm depth (cf. Table 20). For acid sandy soils, measurements from 150 forest stands were used, which were sampled once during the period March to May in 1990 (De Vries and Leeters, 1994). For clay, loess and peat soils measurements from 100 forest stands were used, which were sampled once during the period March to May in 1994 (Klap *et al.*, 1995). For the calcareous sandy soils

data on 50 dune soils (SC-DLO, W. de Vries, pers. comm) were used. For the validation, only the observations for deciduous forest were used.

It is imperative to realize that there exists some crucial differences between the modelled and observed samples (see also De Vries *et al.*, 1994b):

(i) the distribution of the observed soil/vegetation combinations differed from those who were simulated;
(ii) the soil depth of the observations was always 60-100 cm, whereas the soil depth used for the simulations varied from 20-100 cm (cf Table 15);
(iii) SMART2 simulated flux weighted annual average concentrations, whereas the field data were single observations in early spring.

Table 20 Median values of important soil and soil solution parameters as observed at 60-100 cm depth (Obs.) and predicted for 1990 (Mod.) by SMART for deciduous forest

Soil type	N[1]		pH		Al^{3+} ($mol_c\ m^{-3}$)		NH_4^+ ($mol_c\ m^{-3}$)		NO_3^- ($mol_c\ m^{-3}$)	
	Obs.	Mod.	Obs.	Mod.	Obs.	Mod.	Obs.	Mod.	Obs.	Mod.
Sand poor	27	3166	4.0	3.9	0.42	0.63	0.08	0.01	0.25	0.64
Sand rich	28	2283	3.8	4.0	0.49	0.30	0.08	0.00	0.33	0.15
Sand calc.	4	184	7.0	7.0	0.13[2]	0.00	0.06	0.00	0.71	0.00
Peat	30	375	3.8	3.8	0.04	0.05	0.24	0.01	0.02	0.00
Loess	40	72	4.3	4.2	0.18	0.12	0.04	0.00	0.72	0.36
Clay	13	554	6.3	5.9	0.01	0.00	0.00	0.02	0.11	0.41
Clay calc.	17	337	7.4	6.8	0.00	0.00	0.00	0.00	0.06	0.08

1) N represents the number observed and simulated soil/vegetation combinations.
2) The observed Al^{3+} concentration of 0.13 $mol_c\ m^{-3}$ for calcareous sandy soils is anomalous (too high) compared to the pH.

The agreement between the observed and simulated pH was generally good. For clay soils the deviations seemed to be large, but at that high pH values the deviations in terms of H^+ concentration are negligibly small. The agreement for the Al^{3+} concentration appeared to be reasonable (a maximum deviation of 50% for sand poor). The agreement for NH_4^+ and NO_3^- was generally moderate (deviations larger than 50%). For peat soils the calculated NH_4^+ concentration was clearly underestimated. Regarding also a slight underestimation in NO_3^- concentration, there might be an underestimation of the N mineralization or an overestimation of the denitrification. For the poor sandy soils and the clay soils the NO_3^- was clearly overestimated, whereas for rich sandy soils and loess soils it was underestimated. These deviations are an indication that the nitrogen dynamics in SMART2 are modelled or parameterized inadequately. It is likely that the reduction functions for the *MSW* need some improvements. In addition, one should realize that in SMART2 the N mineralization flux, which highly influence the N concentrations, depend largely on the age of the vegetation and the N content in the foliage (cf section 4.4.2). Consequently, nation wide data on the age of the vegetation and the N content in the foliage is required. Finally, it should be stressed that this validation is only limited to deciduous forest with an emphasis on non-calcareous soils. In order to make a validation possible for other vegetation type, additional data gathering on soil and soil solution is required.

4.4.2 Nitrogen mineralization fluxes

In addition to a validation on soil solution concentrations it is worthwhile to validate the calculated N mineralization fluxes as they are an substantial part of the N availability. It is, though, difficult to perform such a validation because N mineralization fluxes depend on: (i) the age of the vegetation, (ii) vegetation management (mowing, grazing or forest harvesting) and (iii) the N flux in atmospheric deposition. The N mineralization fluxes calculated by SMART2 for the year 1990 refer to: (i) relatively mature terrestrial ecosystems (heathlands/grasslands are assumed to be 10 years old; forests are assumed to be 40 years old), (ii) from which no biomass is removed during the simulation period and (iii) with a large atmospheric N input.

Validation should thus focus on data for similar systems. In general, mineralization data are comparatively scarce compared to data on N inputs by litterfall. Although, in a steady-state situation both data can be taken equal. Table 21 summarized N mineralization data. When available, the age of the ecosystem is presented as well.

Table 21 Observed N mineralization rates

Type of ecosystem	Age (a)	N mineralization flux ($kmol_c\ ha^{-1}\ a^{-1}$)	Source
Pine Forest			
Gerritsfles	ca. 60	5.1	Van Dobben *et al.* (1992)[1)]
Tongbersven	ca. 80	5.7	Van Dobben *et al.* (1992)[1)]
Deciduous Forest			
Oak+mixed; Beech	50-100	7 - 8	Tietema (1992)
Oak+mixed; Birch	ca. 45	7 - 8	Van Breemen *et al.* (1988)[1)]
Deciduous forest	varying	3 - 10	Melillo (1981)
Heathland			
Calluna	varying	0.8 - 4.2	Berendse (1990)
Erica	10	0.5 - 3.0	Berendse (1988, 1990)
Erica	30	3.5 - 7.0	Berendse (1988, 1990)
Erica	50	8.2 - 9.1	Berendse (1988, 1990)
Grassland			
chalk grassland	unknown	3.5	Van Dam (1990)
Molinia	10	2 - 3	Berendse (1988)
Molinia	30	6 - 7	Berendse (1988)
Molinia	50	7.6 - 9.3	Berendse (1988)

[1)] These data refers to litterfall fluxes

For heathlands and grasslands, data given by Gorree and Runhaar (1992) for an steady-state situation (mineralization equals litterfall) are 2 - 2.5 $kmol_c\ ha^{-1}\ a^{-1}$. This are, however, calculations that do not include root turnover, which is generally 75% of the total N turnover in these ecosystems (cf. Berendse, 1988). Consequently, the total N mineralization flux would increase up to 8 - 10 $kmol_c\ ha^{-1}\ a^{-1}$ at a steady-state. Note that data on heathlands and grasslands used in SMART2 are based on Berendse (1988), i.e. Erica and Molinia respectively. Validation should thus focus mineralization data by Berendse (1988).

N mineralization fluxes as calculated by SMART2, using the 11 Scenario (constant deposition and seepage), are summarized in Table 22. In Table 22 the N mineralization fluxes in 1990 for forest (Spruce, Pine, Deciduous) referring to a forest of 40 years old and for short vegetation (Heather, Grass) to a site of 10 years old, whereas the values in 2050 can be regarded as a mature ecosystem were litterfall equals mineralization.

Table 22 Calculated N mineralization fluxes

Vegetation type	N mineralization flux ($kmol_c$ ha^{-1} a^{-1}) 1990	2050
Spruce	2.9	4.2
Pine	3.1	4.9
Deciduous	3.4	5.6
Heather	3.4	5.5
Grass	4.4	6.8

In general a comparison is thus difficult. Available mineralization rates compared to assumptions in SMART2 only allows a very approximate comparison. Comparing the model results from Table 22 with observed N mineralization fluxes, it can be concluded that the agreement is generally reasonable. The modelled mineralization fluxes for short vegetation in 2050 (i.e. 70 years old) were comparable with the appropriate ranges in Table 21, whereas the modelled fluxes in 1990 (i.e. 10 years old) are slightly higher than the observed values. It is, however, striking that he modelled mineralization fluxes for forest were always lower than the observed fluxes. This might be an indication that the N litterfall fluxes for forest in SMART2 are underestimated. Data used in SMART2 for the N litterfall flux are a multiplication of average litterfall fluxes with a varying N content depending on the N deposition level. Multiplication of observed ranges in litterfall fluxes and N contents in foliage (Table 23) provides an indication of N mineralization rates at steady-state.

Table 23 N litterfall fluxes

Tree species	Litterfall[1)] (Mkg ha^{-1} a^{-1})	N contents[2)] (%)	N litterfall flux ($kmol_c$ ha^{-1} a^{-1})
(Scots) Pine	0.5 - 8.5[1)]	1.6 - 3.0	0.4 - 12
(Norway) Spruce	1.5 - 7.5[1)]	1.1 - 2.3	0.8 - 8
(Oak) Deciduous	1.6 - 5.6[3)]	2.2 - 3.2	1.6 - 8

1) Data based on a literature compilation for Northern Europe (Reurslag and Berg, 1993)

2) Data for 45 pine stands, 15 spruce stands and 30 oak stands in the Netherlands (Hendriks *et al.*, 1994). Contents refers to contents of the foliage, for the calculation of the litterfall flux a reallocation factor of 0.36 was assumed (cf Table 13)

3) Data based on a review by De Vries *et al.* (1990); Duvigneaud *et al.* (1971) gives ranges of 4.7-7.5 Mkg ha^{-1} a^{-1}

Considering the average maximum litterfall fluxes used in SMART2, i.e. ca. 3 Mkg ha^{-1} a^{-1} for the various tree species (cf. section 3.4), it is obvious that for forest the litterfall fluxes are underestimated, which may result in too low mineralization fluxes in forest.

4.5 Effects on plant species in for nutrient-poor deciduous forest

The effects of a change soil pH (the output variable of the SMART2 model) on species diversity are predicted for plant species of nutrient-poor deciduous forests (i.e. the forest on non-calcareous sandy soils) for 1990 and 2050 using the vegetation model MOVE (Latour and Reiling, 1993)

Characteristic species for nutrient-poor deciduous forest *Quercion Robori-Petraeae* and *Fago-Quercetum* were inferred from Loopstra and Van der Maarel (1984). Ecological response curves of 13 plant species were inferred from Wiertz *et al.* (1992). These species are: *Convallaria majalis, Corydalis claviculata, Deschampsia flexuosa, Hieracium laevigatum, Hieracium umbellatum, Holcus mollis, Luzula piloas, Luzula sylvatica, Melampyrum pratense, Polypodium vulgare, Pteridium aquilinum, Solidago virgauria,* and *Teucrium scorodonia.*

For each species the 10 and 90 percentiles of the species-response curves were calculated. The 10 percentile corresponds with a reduced occurrence probability due to 'shortage or limitation', the 90 percentile due to 'excess or intoxication'. Next, the occurrence probability was plotted for each grid cell. A species was considered probable to occur when the predicted median pH for the non-calcareous sandy soils below deciduous forest in a grid cell was between the 10 percentile and the 95 percentile value of the ecological response curve. The occurrence probability for each grid cell was calculated from the number of the mentioned 13 plant species which are probable to occur.

Figure 9 presents the occurrence probability of species of nutrient-poor deciduous forests on rich an poor sandy soils for 1990, 2010 and 2050. In 1990 the predicted number of species varies on average between 40 and 80% of the considered 13 species. In 2010 this increases to 40 to 100% and in 2050 the occurrence increased in general to 60 to 100% of the species. In some specific areas the predicted percentage of species remained below 20%. In these areas the soil pH is higher than 5.8, which is too high for the species of nutrient-poor deciduous forests.

5 Uncertainties

5.1 Model structure

Although the model structure is possibly an important source of uncertainty, it is very difficult or even impossible to quantify. Uncertainties caused by model structure are due to model assumptions and simplifications that were made. Assumptions and simplifications are made because of insufficient knowledge, to limit data requirements and operational aspects (e.g. applicable at a national scale, which requires model simplification). The lack of knowledge with respect to acidification and nutrient cycling models mainly concerns the dynamics of organic matter, N and Al (De Vries, 1994; Kros *et al.*, 1993). Especially the uncertainties in Al and N dynamics may seriously contribute to the uncertainty in the results of pH and N availability.

With respect to Al dynamics, in SMART2 it is assumed that there is always equilibrium with secondary Al compounds (cf section 2.1), whereas in reality equilibrium occurs only in the subsoil and undersaturation in the topsoil. This assumption will accelerate the depletion of secondary Al compounds and will lead to higher pH and Al^{3+} concentrations in the top soil. The N availability highly depend on the N mineralization flux, which in turn depend on the age of the vegetation, vegetation management (e.g. sod cutting, mowing, grazing and tree harvesting), litterfall and N uptake (cf section 4.4.2). Until now, these aspects are not or not adequately incorporated in the model for all vegetation types. In addition, the reduction functions for pH and *MSW* (cf. section 2.2) as used for N mineralization and the N transformation processes are imperfectly supported by experimental work.

Another aspect that seriously affect the model results is the thickness of the soil compartment. In this study results are calculated for the root zone as a whole, assuming that this compartment is homogeneous. This assumption implies that the calculated concentrations refer to the bottom of the root zone. Generally there is a systematic change in soil solution chemistry and fine root distribution with depth, e.g. the pH and the Al^{3+} concentrations generally decreases with depth, whereas most of the fine roots occur at the top soil. Furthermore, most of the changes in time in soil and soil solution chemistry occur in the top 30 cm (cf section 4.3). Consequently, the assumption of one homogeneous relatively large compartment (up to 1 m) causes that the calculated changes with depth and time are cancelled out. Contrary to SMART, with SMART2 it is possible to assess the effect of soil depth within the root zone (cf section 2.2), which makes it possible to investigate the consequences of soil depth. Finally, the annual time-scale may affect the long-term predictions, but this effect is likely to be small (Kros *et al.*, 1994).

5.2 Input data

The assessment of the uncertainty in model predictions caused by uncertain input data is limited here to the uncertainty in model outputs due to the uncertainty and spatial variability in model input data. For an unbiased uncertainty analysis it is recommended to perform an analysis by performing Monte Carlo simulations followed by a statistical analysis in order to quantify the uncertainty contribution of the model input data (cf Kros *et al.*, 1993, Reinds *et al.*, in prep.). This, however, was not possible and planned within the scope of this research. In order to give at least an indication of the uncertainty due to input data, simulations were performed using the 5th percentile and the 95th percentile values of the soil parameters instead of the median values which where used for the results presented in Chapter 4 (Table 24). Table 24 only present those parameters for which percentile values were available, including initial conditions of state variables, and important model parameters describing the N and Al dynamics like CN_{om} and KAl_{ox}. For all other parameters the same values as given in Table 14 were used. Data were based on the sources mentioned in Chapter 3.

Table 25 presents the median values resulting from using the 5th percentile, 50th percentile (these values are the same as those from Table 17, year 2050) and 95th percentile values from Table 24. All values refer to the root zone below deciduous forest in the year 2050 using Scenario 22. In addition, Table 25 presents percentile values that resulted from the standard simulations for the 22 Scenario (Chapter 4) where median soil parameter values were used, i.e.: 5th percentile (MP05) and the 95th percentile (MP95). Insight into the uncertainty due to uncertainty in generic soil data can be obtained by comparing the P05, P50 and P95 values. Comparing the MP05, P50 and MP95 (Table 25), i.e. the variability in model output using median soil parameter values, provide insight into the variability induced by the spatial variability in atmospheric deposition, hydrology and vegetation types.

Inspecting the P05, P50 and P95 values it is remarkable that the results are not always ranked in an ascending order. This was caused by the fact that a higher value of a specific soil parameter (cf Table 24) may lead to an increase of a specific model output, whereas for another soil parameter the opposite might be true. For example, a higher value for KAl_{ox} results in a higher pH value, cf Eq. (13), whereas a higher value for KH_{ex} results in a lower pH, cf Eq. (7).

Table 24 5th, 50th and 95th percentile for the soil parameters for the seven soil types, related to the depth of the root zone for forest

Parameter (unit)		Percentile	SP	SR	SC	CN	CC	LN	PN
Depth (m)		-	0.70	0.60	0.80	1.00	1.00	1.00	0.50
ρ_{rz}	(g cm^{-3})	P05	1.25	1.22	1.51	1.08	1.08	1.52	0.15
		P50	1.45	1.26	1.62	1.16	1.16	1.52	0.17
		P95	1.48	1.36	1.65	1.38	1.38	1.52	0.31
θ	(m^3 m^{-3})	P05	0.08	0.17	0.037	0.16	0.16	0.28	0.50
		P50	0.13	0.18	0.06	0.27	0.27	0.41	0.84
		P95	0.19	0.23	0.10	0.27	0.27	0.45	0.90
$ctCa_{cb}$	($mmol_c$ kg^{-1})	P05	0.0	0.0	65.8	0.0	5.6	0.0	0.0
		P50	0.0	0.0	182.4	0.0	109.0	0.0	0.0
		P95	0.0	0.0	748.7	0.0	1296.	0.0	0.0
CEC	($mmol_c$ kg^{-1})	P05	8.8	10.0	3.0	103.8	103.8	21.0	334.2
		P50	11.3	41.4	7.9	318.9	318.9	53.7	414.1
		P95	43.0	44.0	27.6	452.6	452.6	149.4	727.5
OM	(kg kg^{-1})	P05	0.01	0.01	0.00	0.03	0.03	0.02	0.38
		P50	0.02	0.06	0.01	0.07	0.07	0.03	0.90
		P95	0.07	0.07	0.01	0.11	0.11	0.06	0.98
CN_{om}	(kg kg^{-1})	P05	13.	13.	8.	9.	9.	13.	13.
		P50	21.	26.	10.	10.	10.	21.	35.
		P95	29.	32.	30.	13.	13.	29.	48.
KAl_{ex}	(log(mol l^{-1}))	P05	-0.5	-0.6	-2.7	-4.3	-4.3	-1.6	-3.5
		P50	0.8	0.2	-1.2	-3.4	-3.4	0.6	-2.1
		P95	1.5	0.7	0.5	-2.9	-2.9	1.2	-1.1
KH_{ex}	(log(mol l^{-1}))	P05	3.5	3.4	4.2	4.0	4.0	3.7	2.5
		P50	4.0	3.8	5.0	6.7	6.7	4.2	3.5
		P95	4.4	4.2	8.5	8.5	8.5	6.4	4.4
KAl_{ox}	(log(mol l^{-1}))	P05	7.4	7.2	7.5	8.5	8.5	7.6	5.1
		P50	8.1	7.9	8.1	9.4	9.4	8.3	6.5
		P95	8.5	8.5	8.6	10.2	10.2	8.9	8.9
$frBC2_{ac}$	(-)	P05	0.04	0.05	0.24	0.66	0.66	0.06	0.21
		P50	0.07	0.06	0.83	0.89	0.89	0.16	0.58
		P95	0.09	0.08	0.99	1.00	1.00	0.89	0.90
$ctAl_{ox}$	($mmol_c$ kg^{-1})	P05	48.0	45.0	5.6	113.9	113.9	82.7	49.1
		P50	84.9	108.5	8.8	196.3	196.3	154.6	101.1
		P95	147.4	131.5	14.3	303.4	303.4	261.9	461.5
SSC	($mmol_c$ kg^{-1})	P05	1.0	0.9	0.1	2.3	2.3	1.7	1.0
		P50	1.7	2.2	0.2	3.9	3.9	3.1	3.1
		P95	2.9	2.6	0.3	6.1	6.1	5.2	9.2

From Table 25 it is clear that the uncertainty in pH and BS induced by input data is nearly negligible for the calcareous sandy soils. Because all the simulated combinations with calcareous soils remained in the carbonate buffer range during the entire simulation period, parameter uncertainty has little or no effect on the pH and base saturation. During the carbonate buffer range the pH was fully determined by the calcite equilibrium, cf Eq. (12) of which the parameters were not included in this analysis. However, when the parameters describing the calcite equilibrium (KCa_{cb} and pCO_2) were included in this analysis, there would be a small effect on pH and base saturation. For the pH at P05 in calcareous clay soils, however, the carbonate content was depleted due to the low initial carbonate content ($ctCa_{cb}$, cf Table 24), resulting in a large uncertainty in pH.

Table 25 Effects of uncertainty in input data on the predicted median pH, N availability and base saturation (BS) in the root zone below deciduous forest for the different soil types in the year 2050. P05, P50, P95 referring to the corresponding median results using the values from Table 24. MP05 and MP95 are the 5th percentile and the 95th percentile resulting from using the median soil parameter values.

Soil type	$N^{1)}$	Percentile	pH	N availability ($kmol_c\ ha^{-1}\ a^{-1}$)	BS (%)
Sand poor	3166	MP05	4.0	5.4	2
		P05	3.9	6.6	8
		P50	4.1	6.7	3
		P95	4.4	6.6	4
		MP95	4.5	7.8	14
Sand rich	2283	MP05	4.1	4.5	4
		P05	4.0	6.5	9
		P50	4.2	6.6	7
		P95	4.5	6.7	7
		MP95	5.0	7.6	80
Sand calc.	184	MP05	7.0	4.9	100
		P05	7.1	5.8	100
		P50	7.1	5.8	100
		P95	7.1	5.5	100
		MP95	7.1	6.4	100
Peat	375	MP05	3.8	3.4	43
		P05	3.4	5.3	22
		P50	3.9	5.2	47
		P95	4.9	5.2	80
		MP95	6.5	7.1	100
Loess	72	MP05	4.2	6.1	9
		P05	4.0	6.5	12
		P50	4.4	6.7	13
		P95	5.9	6.9	86
		MP95	7.1	7.7	100
Clay	554	MP05	6.0	6.2	87
		P05	4.5	6.3	66
		P50	6.0	6.9	88
		P95	6.8	6.9	92
		MP95	6.8	7.9	99
Clay calc.	337	MP05	6.8	5.8	100
		P05	5.9	6.5	99
		P50	6.9	6.5	100
		P95	6.9	6.5	100
		MP95	6.9	7.1	100

[1] N represents the number of evaluated combinations

The uncertainty in pH and base saturation was moderate ($|\Delta\ pH| \leq 0.5$, $|\Delta\ BS| \leq 10\%$) for the poor sandy soils and the rich sandy soils. Both soil types are in the Al buffer range, i.e. proton buffering by dissolution of secondary Al compounds mainly. Consequently the uncertainty in pH (and thereby also in BS) was principally determined by the Al dissolution parameter (KAl_{ox}). Other soil parameters like *CEC* and cation exchange constants hardly influenced the results for the year 2050. At that time the exchange complex was in equilibrium with the deposition, because the deposition was already constant for 40 years (cf Section 3.3.1). However, during a period of deposition changes these parameters seriously influence the model results (cf De Vries *et al.*, 1989).

The uncertainty in pH and base saturation was large for the peat soils, loess soils and clay soils. Because these soil were in the CEC buffer range, the model results are influenced by various soil data such as, *CEC*, $frBC2_{ac}$ and cation exchange constants. Contrary to the sandy calcareous soils, the uncertainty in pH for the calcareous clay soils was large. Due to a low 5 percentile value for $ctCa_{cb}$,

Generally, the uncertainty in N availability was relatively small ($|\Delta N \text{ availability}| \leq 0.5$ $kmol_c$ ha^{-1} a^{-1}). This low uncertainty was mainly caused by the low uncertainty in pH. Because N availability was strongly influenced by the pH through various reduction functions, cf. Eqs (42), (62), (64), the uncertainty in pH was reflected on the uncertainty in N availability. This was confirmed by a larger uncertainty in N availability for clay soils ($|\Delta N \text{ availability}| > 0.5$ $kmol_c$ ha^{-1} a^{-1}), which also had a large uncertainty in pH. It should be stressed that when the uncertainty analysis was not confined to soil parameters alone, the uncertainty in N availability would be much larger, see e.g. the large variation that exits in N litterfall fluxes (cf Section 4.4.2).

Comparison of the MP05 and MP95 values with the P05 and P95 showed that the variability in pH due to spatial variability in model inputs was generally comparable with the uncertainty due to soil input data uncertainty. The variability in N availability due to variability in model inputs was always larger than the uncertainty due to input data uncertainty, which was mainly due to a large spatial variation in N deposition. The spatial variability in base saturation for the non-calcareous sandy soils, peat soils and the loess soils was also larger than the uncertainty due to input data uncertainty, whereas for clay soils the spatial variability was smaller and for calcareous soils there was no difference.

Although the validity of the uncertainty analysis is rather limited, it is likely that the uncertainty in the evaluated model output is comparable with the (spatial) variability of the model results.

6 Conclusions

- Reductions in sulphur and nitrogen deposition lead to an improvement of the abiotic site factors, i.e. a moderate increase in pH and base saturation in non-calcareous soil and a clear decrease in N availability for all soils with forest. For short vegetation (heathland and grassland) there is an increase in N availability.
- The (spatial) variability in all investigated model outputs, i.e. pH, base saturation and N availability is large. The spatial variability in pH and base saturation is linked with the spatial variability in soil type, whereas the spatial variability in N availability is linked with the spatial variability in N deposition.
- N availability highly depends on the age of the vegetation. The development of the short vegetation (heathland and grassland) results in an increase in N availability which is larger than the reductions in N deposition of the evaluated deposition scenario. Consequently, reductions in N deposition not necessarily lead to a reduction in N availability.
- The Seepage Increase Scenario, which is a result of 25% reduction in groundwater abstractions, only affects a very small parts of the Netherlands. Consequently, the effects on the median results of the inspected site factors are negligibly small.
- Effects of the deposition reductions and seepage increase on vegetation show an increase of the average predicted number of species in nutrient-poor deciduous forests varies from between 40 and 80% in 1990 to 60 to 100% in 2050.
- Model predictions of pH and Al^{3+} concentration for deciduous forest on poor sandy soils show a reasonable to good agreement with observations. Model predictions for the NO_3^- and NH_4^+ concentrations show a moderate relationship with the observations.
- An indicative validation on N mineralization fluxes, shows generally a reasonable agreement between calculated fluxes and measured fluxes available from literature. N mineralization fluxes in forest are likely to be underestimated.
- The uncertainty in model results on pH and base saturation is large for the peat soils, loess soils and non-calcareous clay soils, whereas it is moderate for the non-calcareous sandy soils and small for the calcareous soils.
- The influence of uncertainty in soil parameters on the uncertainty in N availability is rather small. However, the overall uncertainty in N availability is likely to be relatively large.

7 Recommendations

The use of a 1 x 1 km^2 grid results in various restrictions with respect to geographical resolution. This resolution is by far to coarse to model ecosystems which forms the topo-sequence within brook-valleys, which have potentially high nature values. Consequently, geographical resolution must be improved for an adequate modelling of site factors in wetlands and brook-valleys. The underlying geographical information used, however, is more detailed e.g., the soil map on a scale of 1 : 50 000, vegetation information on 250 x 250 m^2, but for the presentation the link with geographical location within a 1 x 1 km^2 grid cell is detached. Therefore, it is recommended to improve the spatial resolution of and increase the area which is covered by the model input (deposition, hydrology) and geographical information. This can be achieved by:

- Using deposition values for 1 km^2, which are now available (RIVM, J.W. Erisman pers. comm.).
- Distribution of seepage and *MSW* over the water-table classes within the 1 x 1 km^2 grid cells.
- Extension of the LGM towards the Western part and the southern part of the Netherlands.
- Improvement of groundwater (seepage) quality data. In this study only four quality types were taken into account without making a link with geographical location.

For the site module SMART2 as such, the following improvements and extensions are recommended:

- Improvement and extensions of the N transformations processes and mineralization descriptions.
- Improvement of the reduction functions for pH and water-table.
- Extension of the model towards wetland and bogs.
- Inclusion of vegetation management, like sod cutting, mowing, grazing and tree harvesting. This is especially relevant for the calculation of the N availability, which highly depend on the age of the vegetation and the removal of biomass. The assumption in this study that each distinguished vegetation type has the same age has a predominant influence on the model results. Furthermore, it was assumed that the net production was nil. This was based on the assumption that biomass return to the soil equals biomass production.
- A comprehensive validation of the model SMART2 for all soil and vegetation types, especially for the model output on N availability. The validation in this study was limited to soil solution concentrations under forests on non-calcareous soils.
- Calculations for shallower depth, e.g. 30 cm. In this study calculations are performed for the root zone as a whole (compartments up to 1 m), whereas most of changes in soil and soil solution occur in the top 30 cm, were also most the fine roots occur.
- Performing a complete uncertainty analysis.

Regarding the linkage SMART2-MOVE the relationship between site factors and vegetation effects need to be improved and extended. Until now the link between SMART2 and MOVE was only achieved for the pH under nutrient poor deciduous forest.

References

Alkemade, J.R.M., J. Wiertz and J.B. Latour, 1996. *Calibratie van Ellenberg's milieu-indicatie-getallen aan werkelijk gemeten bodemfactoren.* Bilthoven, RIVM-rapport 711912016.

Aronsson, A., 1980. *Frost hardiness in Scots pine. II Hardiness during winter and spring in young trees of different mineral status.* Studia Forest Suecica 155: 1-27.

Belmans, C., J.G. Wesseling and R.A. Feddes, 1983. *Simulation model of the water balance of a cropped soil providing different types of boundary conditions SWATRE.* J. Hydrol. 63: 27-286.

Berdowski, J.J.M. and R. Zeilinga, 1987. Transition from heathland to grassland: damaging effects of the heather beetle. J. Ecol., 75:159-175.

Berendse, F., H. Oudhof and J. Bol, 1987. *A comparative study on nutrient cycling in wet heathland ecosystems. II. Litter decomposition and nutrient mineralization.* Oecologia 78: 338-348.

Berendse, F., 1988. *De nutriëntenbalans van droge zandgrondvegetaties in verband met de eutrofiëring via de lucht. Deel 1 Een simulatiemodel als hulpmiddel bij het beheer van vochtige heidevelden.* Wageningen, Centrum voor Agrobiologisch Onderzoek, 51 pp.

Berendse, F., 1990. *Organic matter accumulation and nitrogen mineralization during secondary succession in heathland ecosystems.* J. Ecol., 78:413-427.

Bobbink, R. and G.W. Heil, 1993. *Atmospheric deposition of sulphur and nitrogen on heathland ecosystems.* In: R. Aerts and G.W. Heil (Eds.) *Heathlands: Patterns and processes in a changing environment*:25-50.

Bobbink, R., G.W. Heil and M. Scheffers, 1990. *Atmosferische depositie van NO_x in bermvegetaties langs autosnelwegen.* University of Utrecht, Dept. Botanische Oecologie en Evolutiebiologie, 64 pp.

Bobbink, R., M. Hornung and J.G.M. Roelofs, in prep. *The effects of air-borne nitrogen pollutants on vegetation - critical loads*, WHO-guidelines.

Bolsius, E.C.A, J.H.M. Eulderink, C.L.G. Groen, W.B. Harms, A.K. Bregt, M. van der Linden, B.J. Looise, G.J. Maas, E.P. Querner, W.L.M. Tamis, R.W. de Waal, H.P. Wolfert, M. van 't Zelfde, 1994. *Eén digitaal bestand voor de landschapsecologie van Nederland.* Den Haag, VROM, LKN rapport 4.

Boxman, A.W. and H.F.G. Van Dijk, 1988. *Het effect van landbouw ammonium deposities op bos- en heidevegetaties.* Katholieke Universiteit Nijmegen, 96 pp.

Breeuwsma, A., J.P. Chardon, J.F. Kragt and W. De Vries, 1991. *Pedotransfer functions for denitrification.* In ECE 1991, Soil and Groundwater Research Report II 'Nitrate in Soils', Commission of the European Community, Luxembourg: 207-215.

Chemische samenstelling van de neerslag over Nederland, 1985. Bilthoven, KNMI/RIVM Jaarrapport 1985, ISSN 0169-1759, 124 pp.

De Visser, P.H.B. en W. De Vries, 1989. *De gemiddelde waterbalans van bos-, heide- en graslandvegetaties.* Wageningen, Stichting voor Bodemkartering, Rapport nr. 2085, 136 pp.

De Vries, W., 1991. *Methodologies for the assessment and mapping of critical loads and the impact of abatement strategies on forest soils.* Wageningen, the Netherlands, DLO Winand Staring Centre for Integrated Land, Soil and Water Research, Report 46, 109 pp.

De Vries, W., 1993. *De chemische samenstelling van bodem en bodemvocht van duingronden in de provincie Zuid-Holland.* Wageningen, SC-DLO rapport 1993.

De Vries, W., 1994. *Soil response to acid deposition at different regional scales; Field and laboratory data, critical loads and model predictions*, Doctoral thesis Agricultural University, Wageningen, 487 pp.

De Vries, F and J. Denneboom, 1992. *De bodemkaart van Nederland digitaal.* Wageningen, the Netherlands, DLO Winand Staring Centre for Integrated Land, Soil and Water Research, Technical Document 1, 48 pp.

De Vries, W. and E.E.J.M. Leeters, 1994. *Effects of acid deposition on 150 forest stands in the Netherlands. 1. Chemical composition of the humus layer, mineral soil and soil solution.* Wageningen, the Netherlands, DLO Winand Staring Centre for Integrated Land, Soil and Water Research, Report 69.1.

De Vries, W., M. Posch and J. Kämäri, 1989. *Simulation of the long-term soil response to acid deposition in various buffer ranges.* Water Air and Soil Poll. 48: 349-390.

De Vries, W., A. Hol, S. Tjalma en J.C. Voogd, 1990. *Literatuurstudie naar voorraden en verblijftijden van elementen in een bosecosysteem.* Wageningen, DLO-Staring Centrum, Rapport 94, 205 pp.

De Vries, W., J. Klijn and J. Kros, 1994a. *Simulation of the long-term impact of atmospheric deposition on dune ecosystems in the Netherlands.* Journal of Applied Ecology 31: 59-73.

De Vries, W., J. Kros en C. Van der Salm, 1994b. *The long-term impact of three emission-deposition scenarios on Dutch forest soils.* Water Air and Soil Poll. 75:1-35.

De Vries, W., J. Kros and J.C.H. Voogd, 1994c. *Assessment of critical loads and their exceedance on Dutch forests using a multi-layer steady state model.* Water, Air and Soil Pollution 76:407-448.

De Vries, W., G.J. Reinds, M. Posch and J. Kämäri, 1994d. *Long-term soil response to acidic deposition in Europe.* Water Air and Soil Pollution 79:1-32.

De Vries, W., J. Kros and C. Van der Salm, 1995. *Modelling the impact of acid deposition and nutrient cycling in forest soils.* Ecol. Model. 79: 231-254.

De Waal, R.W., 1992. *Bodem- en grondwatertrappen. Toelichting bij het databestand 'BODEMGT' van het LKN-project.* Wageningen, SC-DLO rapport 132.

Duvigneaud, P., P. Kestemont and P. Ambroes, 1971. Productivité primaire des forêts tempérées d'essences feuillues caducifoliées en Europe occidentale. In: P. Duvingneaud (Ed.). *Productivity of forest ecosystems*, Proceedings of the Brussels symposium, Ecology and Conservation 4. UNESCO, Paris, pp 259-270.

Ellenberg, H., H.E. Weber, R. Dull, V. Wirth, W. Werner and D. Paulissen, 1991. *Indicator values of plants in Central Europe.* Erich Goltze, Göttingen.

Erisman, J.W., 1991. *Acid deposition in the Netherlands.* Bilthoven, the Netherlands, National Institute of Public Health and Environmental Protection, Report nr. 723001002, 72 pp.

Food and Agriculture Organization of the United Nations, 1988. *Soil map of the World, revised legend.* World soil resources report 60, FAO, Rome, 138 pp.

Gorree, M. and H. Runhaar, 1992. *Haalbaarheidstudie natuurgerichte normstelling nutriënten.* Centre of Environmental Studies Leiden University, CML Report 88, 45 pp.

Hendriks, C.M.A., 1994. *De verdrogingstoestand en verdrogingsgevoeligheid van het Nederlandse bos.* Wageningen, SC-DLO rapport 289.

Heil, G.W. and W.M. Diemont, 1983. *Raised nutrient levels change heathland into grassland.* Vegetatio 53: 113-120.

Hommel, P.W.F.M., E.E.J.M. Leeters, P. Mekkink and J.G. Vrielink, 1990. *Vegetation changes in the Speulderbos (the Netherlands) during the period 1958-1988.* Wageningen, the Netherlands, DLO Winand Staring Centre for Integrated Land, Soil and Water Research, Report 23.

Janssen, B.H., 1984. *A simple method for calculating decomposition and accumulation of young organic matter.* Plant and Soil: 76 297-304.

Johnson, D.W. and D.E. Todd, 1983. *Relationships among iron, aluminium, carbon, and sulfate in a variety of forest soils.* Soil Sci. Soc. of Am. J. 47: 792-800.

Jongman, R.H.G., C.J.F. Ter Braak and O.F.R. Van Tongeren, 1987. Data analysis in community and landscape ecology. Pudoc, Wageningen, The Netherlands, 299 pp.

Klap, J.M., W. de Vries and E.E.J.M. Leeters, 1995. *Effects of acid atmospheric deposition on the chemical composition of loess, clay and peat soils under forest in the Netherlands - Actual assessments.* Wageningen, SC-DLO report 97.1, 147 pp.

Kleijn, C.E., G. Zuidema and W. De Vries, 1989. *De indirecte effecten van atmosferische depositie op de vitaliteit van Nederlandse bossen. 2. Depositie, bodemeigenschappen en bodemvochtsamenstelling van acht Douglas opstanden.* Wageningen, Stichting voor Bodemkartering, Rapport 2050, 96 pp.

Klijn, F., 1989. *Grondwaterrelaties. Toelichting bij het databestand 'Grondwaterrelaties' van het LKN-project.* Leiden, CML-mededelingen 51/ Wageningen, Stiboka rapport 2107.

Koorevaar, P. G. Menelik and C. Dirksen, 1983. *Elements of soil physics.* Development in Soil Science, 13. Elsevier, Amsterdam, 228 pp.

Kros, J., W. De Vries, P.H.M. Janssen and C.I. Bak, 1993. *The uncertainty in forecasting regional trends of forest soil acidification.* Water Air and Soil Pollut. 66:29-58.

Kros, J., J.E. Groenenberg, W. de Vries and C. van der Salm, 1994. *Uncertainties in long-term predictions of forest soil acidification due to neglecting seasonal variability*, Water Air and Soil Pollut. 79:353-375

Kros, J., C. van der Salm and W. de Vries, In prep. *RESAM, REgional Soil Acidification Model - Model Documentation.* Wageningen, SC-DLO Technical Document 9.

Latour, J.B. en R. Reiling, 1991. *On the Move: concept voor een nationaal effecten model voor de vegetatie (MOVE).* Bilthoven, RIVM rapport 711901003, 23 pp.

Latour, J.B. and R. Reiling, 1993. *MOVE: a multiple-stress model for vegetation*, Sci. Tot. Environ. Supplement, 1513-1526.

Latour, J.B., R. Reiling and J. Wiertz, 1993. 'MOVE: a multiple-stress model for vegetation'. In: J.C. Hooghart and C.W.S. Posthumus (Eds.) *The use of hydro-ecological models in the Netherlands.* Delft, Proceedings and Information / TNO Committee on Hydrological Research: no. 47:53-64.

Melillo, J.M. 1981. 'Nitrogen cycling in deciduous forests'. In: F.E. Clark and T. Rosswall (Eds.) *Terrestrial Nitrogen Cycles.* Stockholm, Ecol. Bull. 33:427-442.

Natuurbeleidsplan, 1989. Ministerie van Landbouw, Natuur en Visserij, Den Haag.

Nederlandse Bosstatistiek, De; Deel 1 De oppervlakte bos van 1980 to 1983, 1985. Den Haag, Centraal Bureau voor de Statistiek, Staatsdrukkerij, 123 pp.

Loopstra, I.L. and Van der Maarel, E.: 1984, *Toetsing van de ecologische soortengroepen in de Nederlandse flora aan het systeem van indicatiewaarden volgens Ellenberg*, De Dorschkamp, Wageningen, report no. 381, 143 pp.

Pastoors, M.J.H., 1992. *Landelijk grondwater model; berekeningsresultaten - Onderzoek effecten grondwaterwinning 12*, Bilthoven, RIVM rapport 714305005.

Pastoors, M.J.H., 1993. *Landelijk grondwater model; conceptuele modelbeschrijving - - Onderzoek effecten grondwaterwinning 10*, Bilthoven, RIVM rapport 714305004.

Posch, M., G.J. Reinds and W. De Vries, 1993. *SMART, Simulation Model for Acidification's Regional Trends*. Model Description and User Manual. Mimeograph Series of the National Board of Waters and the Environment 477, Helsinki, Finland, 43 pp.

Pruyt, M.J., 1984. *Vegetatie, waterhuishouding en bodem in twee vochtige duinvalleien in het Noordhollands duinreservaat*. Castricum, PWN-Rapport 1.2-38, 97 pp.

Reinds, G.J., W. de Vries and J. Kros, in prep. *The uncertainty in predicting trends in forest soil acidification due to the regional variability in soil properties and acid deposition*. Wageningen, SC-DLO Report 111.

Reurslag, A. and B. Berg, 1993. *Förna och organiskt material i skogsmark*. Vattenfall Research Bioenergi, Vällingby, Sweden, Report U(B) 1993/2.

Reuss, J.O. and D.W. Johnson, 1986. *Acid deposition and the acidification of soils and waters*. Ecological Studies 59. Springer-Verlag, Berlin, Germany, 119 pp.

Roelofs, J.G.M., A.J. Kempers, A.L.F.M. Houdijk and J. Jansen, 1985. *The effect of airborne ammonium sulphate on Pinus nigra var. maritima in the Netherlands*. Plant and Soil, 84: 45-56.

Schaminee, J.H.J., V. Westhoff and G. van Wirdum, 1989. Naar een nieuw overzicht van de plantengemeenschappen van Nederland. De Levende Natuur 90: 204-209.

Thunnissen, H.A.M., R. Olthof, P. Getz and L. Vels, 1992. *Grondgebruiksdatabank van Nederland vervaardigd met behulp van Landsat Thematic Mapper opnamen*. Wageningen, SC-DLO rapport 168, 225 pp.

Ter Braak, C.J.F. and N.J.M. Gremmen, 1987. *Ecological amplitudes of plant species and the internal consistency of Ellenberg's indicator values for moisture*. Vegetatio 69: 79-87.

Tietema, A., 1992. *Nitrogen cycling and soil acidification in forest ecosystems in the Netherlands.* Ph.D. thesis, University of Amsterdam, the Netherlands, 139 pp.

Tinhout, A. and M.J.A. Werger, 1988. *Fine roots in a dry Calluna heathland.* Acta. Bot. Neerl. 37(2): 225-230.

Ulrich, B., 1983. *Interactions of forest canopies with atmospheric constituents: SO_2, alkali and earth alkali cations and chloride.* In: B. Ulrich and J. Pankrath (Eds.), Effects of air pollutants in forest ecosystems. Reidel Publ. Co., Dordrecht, the Netherlands: 33-45.

Van Amstel, A.R., L.C. Braat en A.C. Garritsen, 1989. *Verdroging van natuur en landschap in Nederland: beschrijving en analyse.* 's-Gravenhage, Ministerie van Verkeer & Waterstaat.

Van Breemen, N., P.A. Burrough, E.J. Velthorst, H.F. Van Dobben, T. De Wit, T.B. De Ridder and H.F.R. Reynders, 1982. *Soil acidification from atmospheric ammonium sulfate in forest canopy throughfall.* Nature 299: 548-550.

Van Breemen, N., C.T. Driscoll and J. Mulder, 1984. *Acidic deposition and internal proton sources in acidification of soils and waters.* Nature 307: 599-604.

Van Dam, D., 1990. *Atmospheric deposition and nutrient cycling in chalk grassland.* Thesis University of Utrecht, 119 pp.

Van Dobben, H.T., J. Mulder, H. Van Dam and H. Houweling, 1992. *Impact of atmospheric deposition on the biogeochemistry of Moorland pools and surrounding terrestial environment.* Agricultural Research Report 93, PUDOC Scientific Publishers, Wageningen, the Netherlands, 232 pp.

Van der Sluijs, P., 1990. 'Grondwatertrappen'. In: W.P. Locher and H. de Bakker (Eds.) *Bodemkunde van Nederland, deel 1, Algemene Bodemkunde.* Den Bosch, Malmberg: 167-180.

Van Veen, J.A., 1977. *The behaviour of nitrogen in soil: a computer simulation model.* Thesis Free University Amsterdam, 164 pp.

Van Wirdum, G., 1991. *Vegetation and hydrology of floating rich-fens.* Thesis University of Amsterdam, 310 pp.

Vermeer, J.G. and F. Berendse, 1983. *The relationship between nutrient availability, shoot biomass and species richness in grassland and wetland communities.* Vegetatio, 53:121-126.

Wiertz, J., J. van Dijk and J.B. Latour, 1992. *De MOVE-vegetatie module: De kans op voorkomen van 700 plantesoorten als functie van vocht, pH, nutrienten en zout.*, Wageningen, IBN-DLO report no. IBN 92/24/Bilthoven, RIVM report 711901006, 138 pp.

Unpublished sources

Hootsmans, R.M. and J.G. van Uffelen, 1991. *Assessment of input data for a simple mass balance model to map critical acid loads for Dutch forest soils.* DLO-Staring Centrum, Interne Mededeling 133, 97 pp.

Janssen, B.H., 1983. *Organische stof en bodemvruchtbaarheid.* Landbouwuniversiteit, Wageningen, Intern Rapport, 215 pp.

Rosén, K., 1990. *The critical load of nitrogen to Swedish forest ecosystems.* Uppsala, Sweden, Swedish University of Agriculture Science, Department of forest soils. Internal Report, 15 pp.

Weterings, M., 1989. *Verzuring van radebrikgronden onder verschillend historisch gebruik.* Wageningen, Agricultural University, Internal report, 61 pp.

Annex 1 List of symbols used in the process descriptions in the SMART2 model

Symbol	Explanation	Unit
θ	volumetric moisture content of the soil	$m^3\ m^{-3}$
ρ_{iz}	bulk density of the soil in the zone where N immobilization occurs	$kg\ m^{-3}$
ρ_{rz}	bulk density of the soil in the root zone	$kg\ m^{-3}$
a_{de}	soil dependent parameter for determination of $rf_{de\ MSW}$	-
age_{lt}	age of the site	a
age_{vg}	age of the vegetation	a
Am_{lt}	amount of litter	$kg\ ha^{-1}$
Am_{lf}	actual amount of litterfall	$kg\ ha^{-1}\ a^{-1}$
$Am_{lf\ mx}$	maximum amount of litterfall	$kg\ ha^{-1}\ a^{-1}$
AmN_{iz}	amount of nitrogen in the zone where N immobilization occurs	$mol_c\ kg^{-1}$
Am_{st}	actual amount of stems and branches	$kg\ ha^{-1}$
$Am_{st\ mx}$	maximum amount of stems and branches	$kg\ ha^{-1}$
a_{ni}	soil dependent parameter for determination of $rf_{ni\ MSW}$	-
b_{ni}	soil dependent parameter for determination of $rf_{ni\ MSW}$	m^{-1}
CEC	cation exchange capacity	$mol_c\ kg^{-1}$
CN_{cr}	critical C/N ratio of the soil	$g\ g^{-1}$
CN_{mn}	minimum C/N ratio of the soil	$g\ g^{-1}$
CN_{om}	C/N ratio of the soil	$g\ g^{-1}$
$ctAl_{ox}$	content of Al in secondary Al compounds in the soil	$mol_c\ kg^{-1}$
$ctCa_{cb}$	amount of Ca in carbonates in the soil	$mol_c\ kg^{-1}$
ctC_{iz}	organic carbon content in the zone where N immobilization occurs	$mol_c\ kg^{-1}$
$ctN_{lv\ mx}$	maximum N content in leaves	$mol_c\ kg^{-1}$ or %
$ctN_{lv\ mn}$	minimum N content in leaves	$mol_c\ kg^{-1}$ or %
ctX_{lv}	nutrient content in leaves of ion X (N, K^+, BC^{2+})	$mol_c\ kg^{-1}$ or %
ctX_{sh}	nutrient content in shoot of ion X (N, K^+, BC^{2+})	$mol_c\ kg^{-1}$ or %
$C_{½}$	half-saturation constant for sulphate sorption	$mol_c\ m^{-3}$
DA_{mo}	dissimilation to assimilation ratio of decomposing microbes	-
dt	time step	a
fdd	dry deposition factor	-
fr_{de}	actual denitrification fraction	-
$fr_{de\ mx}$	maximum denitrification fraction	-
fr_{int}	interception fraction	-
fr_{mi}	actual mineralization fraction fresh litter	-
$fr_{mi\ mx}$	maximum mineralization fraction fresh litter	-
fr_{ni}	actual nitrification fraction	-
$fr_{ni\ mx}$	maximum nitrification fraction	-
frN_{re}	reallocation of N fraction before litterfall	-
$fr_{rt\ lt}$	fraction roots in the litter layer	-
fr_{ru}	cumulative transpiration fraction	-
frX_{ac}	fraction of ion X (BC^{2+}, Al^{3+}, H^+) on the adsorption complex	-
frX_{fe}	foliar exudation fraction	-
frX_{fu}	foliar uptake fraction	-
frX_{le}	leaching fraction from fresh litter of ion K^+ and BC^{2+}	-
frX_{le}	leaching fraction from fresh litter of ion K^+ and BC^{2+}	-
K_a	dissociation constant for organic acids	$mol_c\ m^{-3}$
KAl_{ex}	selectivity constant for Al^{3+}/BC^{2+} exchange	$mol_c^{-1}\ m^3$
KAl_{ox}	dissolution constant for Al-hydroxide	$mol_c^{-2}\ m^6$
KBC_{cb}	dissolution constant for calcium carbonate	$(mol_c\ m^{-3})^3\ hPa^{-1}$
KCO_2	dissociation constant for CO_2	$mol_c^2\ m^{-6}\ hPa^{-1}$
k_{gl}	growth rate constant for logistic growth	$kg\ ha^{-1}\ a^{-1}$

Symbol	Explanation	Unit
KH_{ex}	selectivity constant for H^+/BC^{2+} exchange	$mol_c\ m^{-3}$
kr_{mi}	actual mineralization rate constant old litter	a^{-1}
$kr_{mi\ mx}$	maximum mineralization rate constant old litter	a^{-1}
MHW	mean highest water-table	m
MLW	mean lowest water-table	m
ncf	*nutrient cycling factor (ratio above ground N cycle/below ground N cycle)*	-
N_{de}	denitrification flux	$mol_c\ m^{-2}\ a^{-1}$
N_{im}	N immobilization flux	$mol_c\ m^{-2}\ a^{-1}$
$N_{le\ mn}$	Minimum N leaching flux	$mol_c\ m^{-2}\ a^{-1}$
N_{ni}	nitrification flux	$mol_c\ m^{-2}\ a^{-1}$
$N_{td\ mx}$	total N deposition above which $ctN_{lv} = ctN_{lv\ mx}$	$mol_c\ m^{-2}\ a^{-1}$
$N_{td\ mn}$	total N deposition below which $ctN_{lv} = ctN_{lv\ mn}$	$mol_c\ m^{-2}\ a^{-1}$
OM	organic matter content	$g\ g^{-1}$
P	precipitation	$m\ a^{-1}$
pCO_2	partial CO_2 pressure in the soil	hPa
PE	precipitation excess	$m\ a^{-1}$
$rf_{mi\ MSW}$	reduction fraction of the mineralization rate for the water-table	-
$rf_{mi\ CN}$	reduction fraction of the mineralization rate for N content	-
$rf_{ni\ MSW}$	reduction fraction of the mineralization rate for the water-table	-
$rf_{de\ MSW\ mn}$	minimum denitrification reduction fraction for the water-table	-
$rf_{de\ pH}$	reduction fraction of the denitrification fraction for pH	-
$rf_{de\ MSW}$	reduction fraction of the denitrification fraction for the water-table	-
$rf_{ni\ pH}$	reduction fraction of the nitrification fraction for pH	-
$rf_{ni\ MSW\ mn}$	minimum nitrification reduction fraction for the water-table	-
$rf_{mi\ pH}$	reduction fraction of the mineralization rate for pH	-
ru_{exp}	root uptake exponent	-
Se	seepage flux	$m\ a^{-1}$
$ctSO_{4\ ac}$	Sulphate content at the adsorption complex	$mmol_c\ kg^{-1}$
SSC	Sulphate adsorption capacity	$mmol_c\ kg^{-1}$
t	time	yr
$t_{½}$	half-life time parameter of logistic growth function	a
T_{iz}	thickness of the zone where N mobilization occurs	m
Tr	transpiration flux	$m\ a^{-1}$
T_{rz}	thickness of the root zone	m
X_{fe}	foliar exudation flux of ion X (K^+, BC^{2+})	$mol_c\ m^{-2}\ a^{-1}$
X_{fu}	foliar uptake flux of ion X (NH_4^+, H)	$mol_c\ m^{-2}\ a^{-1}$
X_{gu}	growth uptake flux of element X (N, K^+, BC^{2+})	$mol_c\ m^{-2}\ a^{-1}$
X_{in}	input flux of ion X (SO_4^{2-}, NO_3^-, NH_4^+, Cl^-, $RCOO^-$, K^+, Na^+, BC^{2+}, HCO_3^-, Al^{3+})	$mol_c\ m^{-2}\ a^{-1}$
X_{int}	interaction flux of ion X (SO_4^{2-}, NO_3^-, NH_4^+, Cl^-, $RCOO^-$, K^+, Na^+, BC^{2+}, HCO_3^-, Al^{3+})	$mol_c\ m^{-2}\ a^{-1}$
X_{la}	lateral output flux of ion X (SO_4^{2-}, NO_3^-, NH_4^+, Cl^-, $RCOO^-$, K^+, Na^+, BC^{2+}, HCO_3^-, Al^{3+})	$mol_c\ m^{-2}\ a^{-1}$
X_{lf}	litterfall flux of ion X (NH_4^+, $RCOO^-$, K^+, BC^{2+})	$mol_c\ m^{-2}\ a^{-1}$
X_{mi}	mineralization flux old litter of ion X (NH_4^+, $RCOO^-$, K^+, BC^{2+})	$mol_c\ m^{-2}\ a^{-1}$
$X_{mi\ fl}$	mineralization flux fresh litter of ion X (NH_4^+, $RCOO^-$, K^+, BC^{2+})	$mol_c\ m^{-2}\ a^{-1}$
$X_{rd\ ms}$	root decay flux in the mineral soil of ion X (NH_4^+, $RCOO^-$, K^+, BC^{2+})	$mol_c\ m^{-2}\ a^{-1}$
$X_{rd\ lt}$	root decay flux in the litter layer of ion X (NH_4^+, $RCOO^-$, K^+, BC^{2+})	$mol_c\ m^{-2}\ a^{-1}$
X_{se}	seepage flux of ion X (SO_4^{2-}, NO_3^-, NH_4^+, Cl^-, K^+, Na^+, BC^{2+}, HCO_3^-, Al^{3+})	$mol_c\ m^{-2}\ a^{-1}$
X_{sen}	net seepage flux of ion X (SO_4^{2-}, NO_3^-, NH_4^+, Cl^-, $RCOO^-$, K^+, Na^+, BC^{2+}, HCO_3^-, Al^{3+})	$mol_c\ m^{-2}\ a^{-1}$
X_{td}	total deposition of element X (SO_4^{2-}, N, K^+, Na^+, BC^{2+})	$mol_c\ m^{-2}\ a^{-1}$
X_{we}	weathering flux of base cation X (Na^+, K^+, BC^{2+})	$mol_c\ m^{-3}\ a^{-1}$
z	depth	m
[X]	concentration of ion X (SO_4^{2-}, NO_3^-, K^+, Na^+, BC^{2+}, HCO_3^-, Al^{3+} and H^+) in soil solution	$mol_c\ m^{-3}$

Annex 2 The model area as used for the groundwater modelling

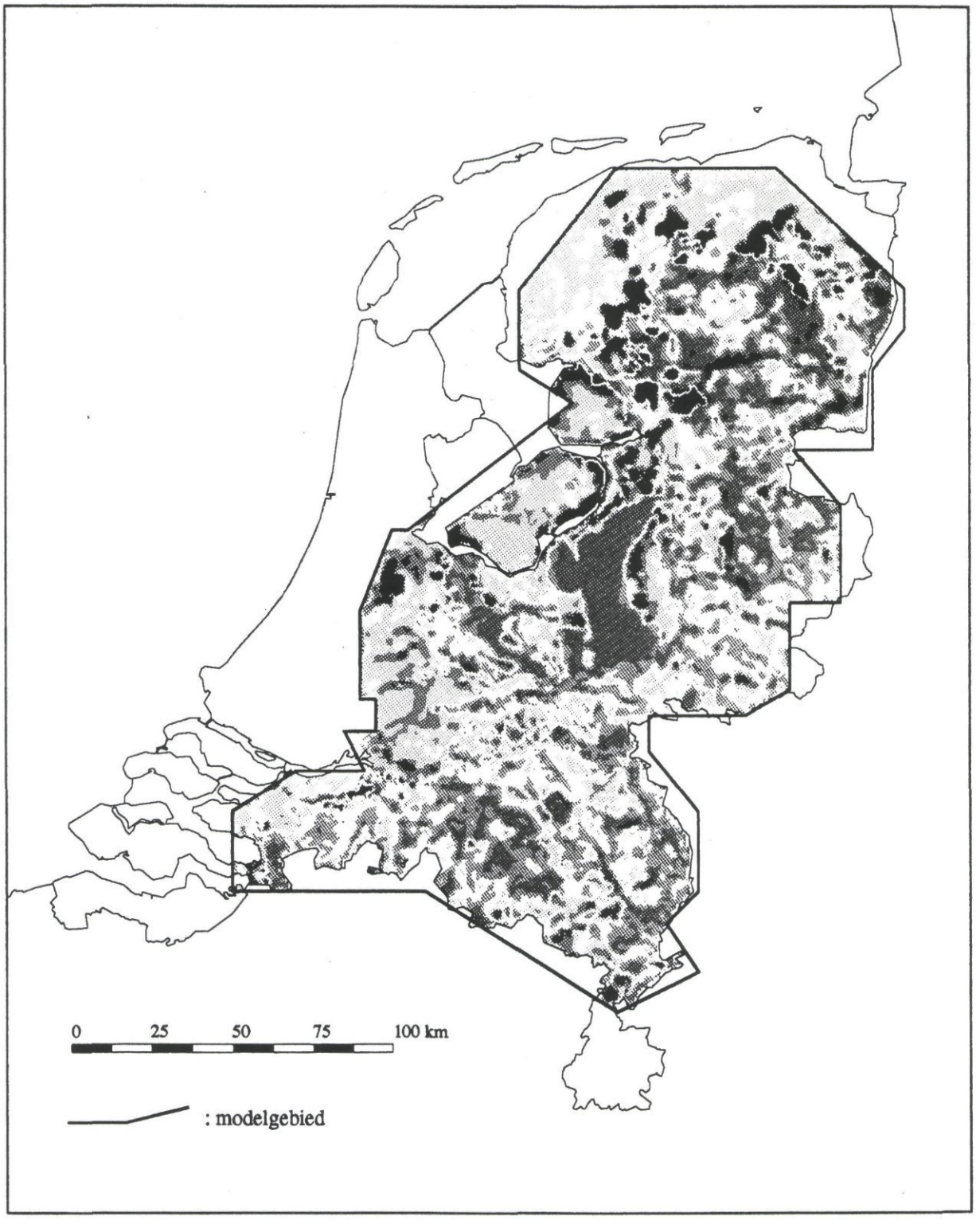

Gebieden met kwel [mm/dag]

- 0.0 - 0.5
- 0.5 - 1.0
- 1.0 - 2.0
- > 2.0

Gebieden met infiltratie [mm/dag]

- 0.0 - 0.5
- 0.5 - 1.0
- 1.0 - 2.0
- > 2.0

Annex 3 Relation used soil types and the 1 : 50 0000 soil map code

Sand			Clay		Loess	Peat
non-calcareous		calcareous	non-calcareous	calcareous		
poor	rich					
zV	uV	EZ..A	EK	pMn..A	EL	vWz
zW	Wpp	pZg..A	kWp	Mv..A	BLn	vWp
iV	uWp	Zn..A	kWz	Rv..A	BLh	hVh
iW	iWzp	Zd..A	Wo	Mo..A	BLd	hEV
Y	uWz	Zb..A	Wg	Ro..A	BLb	aVb
Hn	zWz	Sn..A	pV	Mn..A	pLn	aEV
Hd	EZg	AZW0A	kV	Rn..A	Ln	Vo
pZ	bEZn	AZW1A	BKn	Rd..A	Lnd	V
tZd	zEZ	AZW5A	BKh	AEm.A	Lnh	AAP
cZd	cY		BKd	AEp.A	Lh	ABv
Zn	cHn		MOo	AZW6A	Ld	AP
Zd	cHd		MOb	AZW7A	Ldd	AVk
Zb	pZg		ROo	AZW8A	Ldh	AVo
MZ	BZn		ROb		ABI	AWv
FG	BZd		pMn..C		AHc	
G	BZh		Mv..C		AHl	
AB	MZkH		Rv..C		AHz	
AD	ABz		Mo..C			
AS	AFz		Ro..C			
AZ	AK		Mn..C			
excl...23[1]	AQ		Rn..C			
	AR		Rd..C			
	incl...23		bRn..C			
			gMn..C			
			kMn..C			
			Md			
			pMv			
			pRv			
			pRn			
			pMo			
			pMd			
			pKRn			
			KRn			
			KRd			
			MA			
			MK			
			FK			
			KM			
			KK			
			KS			
			KX			
			KT			
			AAK			
			ABk			
			AEk			
			AEm			
			AFk			

[1] All codes with digit code ..23 have been moved to the class sand rich

Continuation

Sand			Clay		Loess	Peat
non-calcareous		calcareous	non-calcareous	calcareous		
poor	rich					
			AGm.C			
			AHa			
			AHb			
			AHk			
			AHs			
			AHt			
			AHv			
			ALu			
			AM			
			AMm			
			AO			
			AWg			
			AWo			